iScience

CellPress
OPEN ACCESS

Article

Opposing effects of chronic glucagon receptor agonism and antagonism on amino acids, hepatic gene expression, and alpha cells

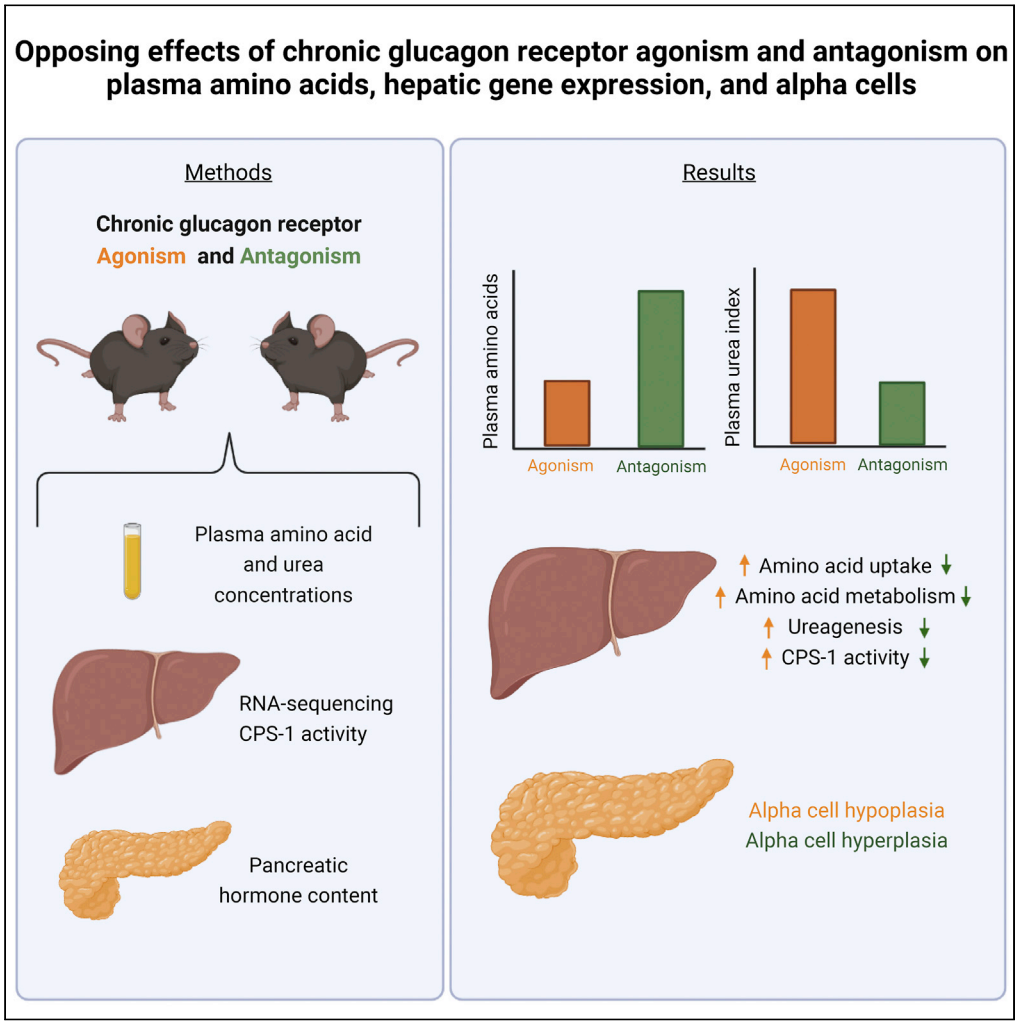

Emilie Elmelund, Katrine D. Galsgaard, Christian D. Johansen, ..., Trisha J. Grevengoed, Jens J. Holst, Nicolai J. Wewer Albrechtsen

nicolai.albrechtsen@sund.ku.dk

Highlights

Glucagon receptor agonism increases amino acid catabolism and hepatic CPS-1 activity

Glucagon receptor signaling regulates the number of pancreatic alpha cells

Glucagon regulates the hepatic transcription of genes involved in amino acid metabolism

Elmelund et al., iScience 25, 105296
November 18, 2022
https://doi.org/10.1016/j.isci.2022.105296

iScience

CellPress
OPEN ACCESS

Article

Opposing effects of chronic glucagon receptor agonism and antagonism on amino acids, hepatic gene expression, and alpha cells

Emilie Elmelund,[1,7] Katrine D. Galsgaard,[1,2,7] Christian D. Johansen,[1,3] Samuel A.J. Trammell,[1] Anna B. Bomholt,[1] Marie Winther-Sørensen,[1,3] Jenna E. Hunt,[1,2] Charlotte M. Sørensen,[1] Thomas Kruse,[4] Jesper F. Lau,[4] Trisha J. Grevengoed,[1] Jens J. Holst,[1,2,6] and Nicolai J. Wewer Albrechtsen[1,3,5,6,8,10,*]

SUMMARY

The pancreatic hormone, glucagon, is known to regulate hepatic glucose production, but recent studies suggest that its regulation of hepatic amino metabolism is equally important. Here, we show that chronic glucagon receptor activation with a long-acting glucagon analog increases amino acid catabolism and ureagenesis and causes alpha cell hypoplasia in female mice. Conversely, chronic glucagon receptor inhibition with a glucagon receptor antibody decreases amino acid catabolism and ureagenesis and causes alpha cell hyperplasia and beta cell loss. These effects were associated with the transcriptional regulation of hepatic genes related to amino acid uptake and catabolism and by the non-transcriptional modulation of the rate-limiting ureagenesis enzyme, carbamoyl phosphate synthetase-1. Our results support the importance of glucagon receptor signaling for amino acid homeostasis and pancreatic islet integrity in mice and provide knowledge regarding the long-term consequences of chronic glucagon receptor agonism and antagonism.

INTRODUCTION

The hormone glucagon is secreted from pancreatic alpha cells. Glucagon increases hepatic glucose production, and increased plasma levels of glucagon (hyperglucagonemia) in patients with type 2 diabetes (Raskin and Unger, 1978) importantly contribute to hyperglycemia (Kazda et al., 2016). This makes the glucagon receptor an appealing target in type 2 diabetes treatment (Pearson et al., 2016). Moreover, glucagon has numerous additional metabolic functions (Habegger et al., 2010; Muller et al., 2017), indicating that the role of glucagon in metabolic diseases extends further than glucose metabolism. Hyperglucagonemia is also seen in subjects with non-alcoholic fatty liver disease (NAFLD) (Junker et al., 2016), an increasing health burden currently affecting >25% of the overall adult population in the United States (Noureddin et al., 2022). Recently, a feedback system called the liver-alpha cell axis, in which glucagon increases hepatic amino acid uptake and ureagenesis while circulating amino acids stimulate alpha cell secretion and growth (Solloway et al., 2015; Dean et al., 2017; Kim et al., 2017; Galsgaard et al., 2018) has gained increasing attention. Experimental or pharmacological disruption of the liver-alpha cell axis impairs hepatic amino acid metabolism, resulting in hyperaminoacidemia, and evidence now suggest that the liver-alpha cell axis may be disrupted by NAFLD (Winther-Sorensen et al., 2020; Suppli et al., 2020). Hyperaminoacidemia increases pancreatic glucagon secretion, leading to hyperglucagonemia and alpha cell hyperplasia (Solloway et al., 2015; Galsgaard et al., 2018; Dean et al., 2017), forming a vicious circle of increasing levels of glucagon and amino acids. Alpha cell hyperplasia depends on the up-regulation of the pancreatic amino acid transporter Slc38a5 (Kim et al., 2017) and on the kinase mammalian Target of Rapamycin (mTOR), a key regulator of proliferation and growth (Solloway et al., 2015) and may specifically involve L-glutamine (Dean et al., 2017). *Gcgr*$^{-/-}$ mice have decreased hepatic expression of genes related to amino acid metabolism and ureagenesis (Kim et al., 2017; Solloway et al., 2015; Winther-Sorensen et al., 2020), while glucagon increases expression of ureagenesis enzymes (Bobe et al., 2009), but the specific mechanisms by which glucagon drives hepatic amino acid metabolism are still unclear. Insight in how prolonged alterations of glucagon receptor activity affect the liver-alpha cell axis is also lacking.

[1]Department of Biomedical Sciences, Faculty of Health and Medical Sciences, University of Copenhagen, 2200 Copenhagen, Denmark

[2]Novo Nordisk Foundation Center for Basic Metabolic Research, Faculty of Health and Medical Sciences, University of Copenhagen, 2200 Copenhagen, Denmark

[3]Novo Nordisk Foundation Center for Protein Research, Faculty of Health Sciences, University of Copenhagen, 2200 Copenhagen, Denmark

[4]Novo Nordisk A/S, Research Chemistry, Novo Nordisk Park, 2760 Måløv, Denmark

[5]Department of Clinical Biochemistry, Bispebjerg & Frederiksberg Hospitals, University of Copenhagen, 2400 Bispebjerg, Denmark

[6]senior author

[7]These authors contributed equally

[8]Twitter: @nicwin98

[10]Lead contact

*Correspondence: nicolai.albrechtsen@sund.ku.dk

https://doi.org/10.1016/j.isci.2022.105296

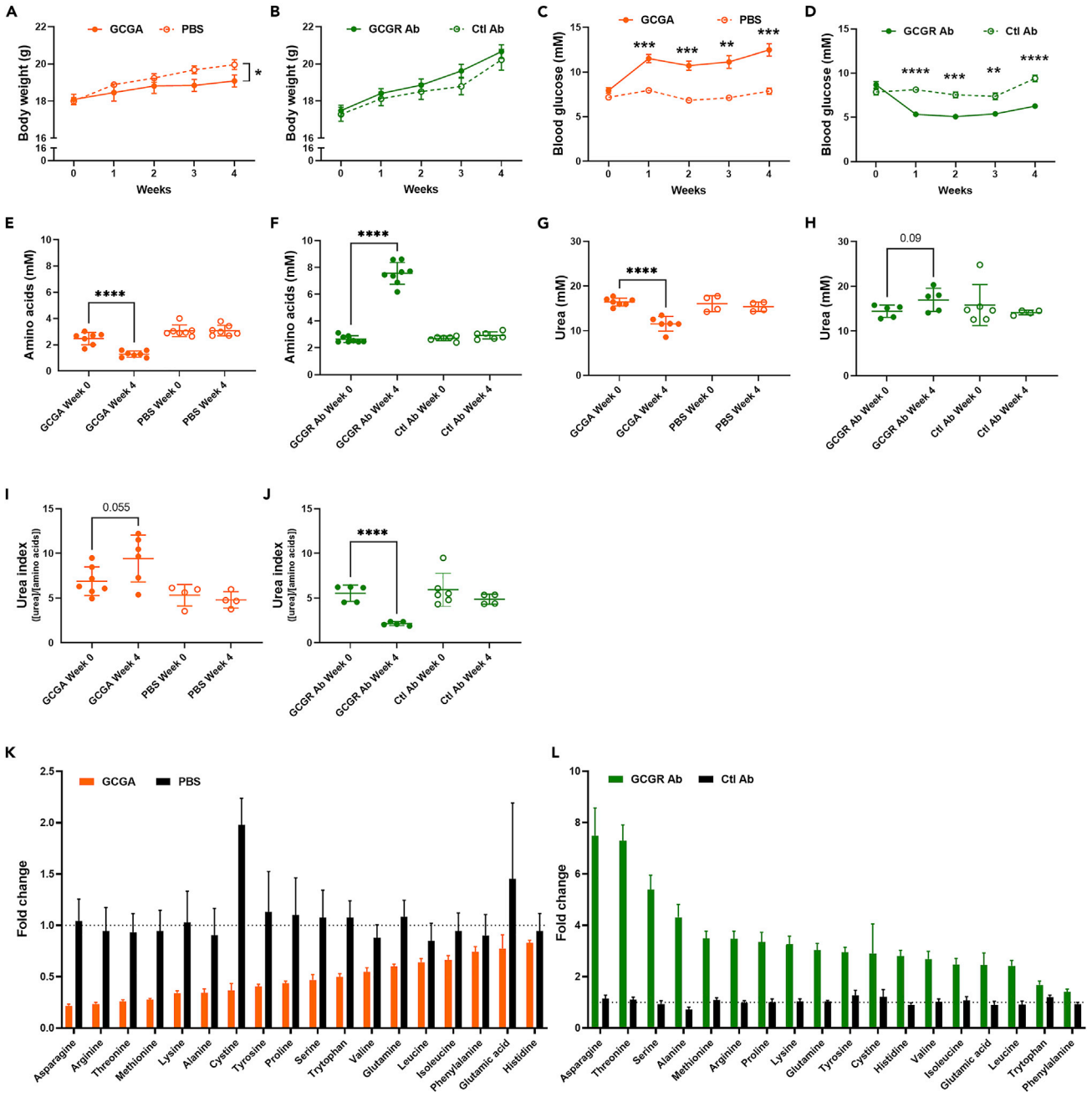

Figure 1. Chronic activation and inhibition of glucagon receptor signaling, respectively, enhances and reduces amino acid metabolism in female mice

(A and B) Weekly body weight in female C57BL/6JRj mice treated (A) twice daily for four weeks with a long-acting glucagon analog (GCGA, NNC9204-0043, 1.5 nmol/kg body weight) or PBS +1% BSA (PBS) or (B) treated once weekly for four weeks with a glucagon receptor antibody (GCGR Ab, REGN1193, Regeneron, 10 mg/kg body weight) or control antibody (Ctl Ab, REGN1945, Regeneron, 10 mg/kg body weight).

(C and D) Weekly blood glucose in mice treated with (C) GCGA or PBS or (D) GCGR Ab or Ctl Ab.

(E and F) Total plasma amino acid levels in mice treated with (E) GCGA or PBS or (F) GCGR Ab or Ctl Ab.

(G and H) Plasma urea levels in mice treated with (G) GCGA or PBS or (H) GCGR Ab or Ctl Ab.

(I and J) Calculated urea index ([urea]/[amino acids]) for mice treated with (I) GCGA or PBS or (J) GCGR Ab or Ctl Ab.

(K and L, NB! the y-axes differ) Fold change of individual amino acids at week four relative to baseline in mice treated with (K) GCGA or PBS or (L) GCGR Ab or Ctl Ab. Glycine was not measured in the samples, and aspartic acid was not detected in any of the samples. The fold changes in the treatment groups (GCGA and GCGR Ab) were statistically significant ($p < 0.05$) from week zero to week four for all amino acid measurements, except for glutamic acid in the

Figure 1. *Continued*

GCGA-treated mice (p = 0.056). The corresponding absolute plasma concentrations and p-values are available in Table S1. All plasma samples were taken prior to injection. The mice were seven weeks old at the beginning of the study. Data in (A–D) and (K and L) are presented as mean ± SEM, n = 3–7. Data in (E–J) are presented as mean ± SD, n = 4–8. p-values (A) by unpaired t-tests of Δblood glucose concentrations, (C and D) by two-way ANOVA, and (E–J) by unpaired t-tests, *p < 0.05, **p < 0.01, ***p < 0.001, ****p < 0.0001.

In this study, we investigated the effects of chronic activation and inhibition of glucagon receptor signaling on the liver-alpha cell axis in female mice. We hypothesized that chronically increased glucagon receptor signaling, made possible by the application of a long-acting glucagon analog, would enhance amino acid metabolism and ureagenesis, while chronically impaired glucagon receptor signaling, brought about by a glucagon-receptor antibody, would have opposite effects. In addition, we assessed pancreatic changes, hypothesizing that chronic glucagon antagonism would produce alpha cell hyperplasia and that glucagon agonism would have opposite effects.

RESULTS

Chronic activation and inhibition of glucagon receptor signaling in female mice, respectively, enhances and reduces amino acid metabolism

We initially evaluated plasma glucagon levels after the administration of a long-acting glucagon analog (GCGA, NNC9204-0043, Novo Nordisk A/S, 3 nmol/kg) once or twice during a 24-h period. The long-acting glucagon analog had the following amino acid substitutions compared to native glucagon: 17K, 18K, 21E, 24K, 27L. A long half-life in plasma of the analog was secured by the attachment of a C18 fatty diacid side-chain at the lysine in position 24 (Figure S1), identical to the once-weekly glucagon-like peptide 1 (GLP-1) receptor agonist semaglutide (Lau et al., 2015). The amino acid substitutions together with the sidechain resulted in a biophysically stable compound suitable for *in vivo* experiments. After a single administration of GCGA, plasma glucagon levels returned to baseline after 24 h, whereas two administrations resulted in persistently elevated glucagon levels (representing the sum of endogenous glucagon and GCGA) throughout the 24 h (Figure S1). Two daily doses of GCGA were thus deemed optimal for chronic agonism of the glucagon receptor.

We subsequently chronically agonized or antagonized the glucagon receptor in female C57BL/6JRj mice and investigated the effects on the liver-alpha cell axis. Thirty-two mice were randomized into four groups of eight. One group of mice was treated twice daily with GCGA (1.5 nmol/kg body weight) while the second group received vehicle (the diluent for GCGA; phosphate-buffered saline (PBS) + 1% bovine serum albumin, this group is from here on referred to as PBS) twice daily. A third group was treated once weekly with a glucagon receptor antibody (GCGR Ab, REGN1193, 10 mg/kg body weight, Regeneron) (Okamoto et al., 2015) while the fourth group received a control antibody (Ctl Ab, REGN1945, 10 mg/kg body weight, Regeneron) once weekly. After four weeks of treatment, mice treated with GCGA had gained less weight than PBS-treated mice (1.0 ± 0.2 vs. 1.96 ± 0.3 g, p = 0.01) (Figure 1A), while there was no difference in the weight gain between GCGR Ab-treated mice and Ctl Ab-treated mice (Figure 1B). After one week, GCGA treatment increased blood glucose levels (Figure 1C), and GCGR Ab treatment decreased blood glucose levels (Figure 1D), and both effects persisted throughout the treatment period. At week four, plasma levels of total amino acids were reduced to 52% of the baseline (the blood samples taken at week zero, prior to treatment) (Figure 1E, p < 0.0001), while in mice treated with GCGR Ab, plasma levels of total amino acids were 2.9-fold increased, compared to baseline (Figure 1F, p < 0.0001). Plasma urea levels decreased in mice treated with GCGA (Figure 1G, p < 0.0001) and increased in mice treated with GCGR Ab (Figure 1H, p = 0.09). Suspecting that these results reflected the reduced (GCGA, Figure 1E) and increased (GCGR Ab, Figure 1F) amino acid availability for ureagenesis, we calculated an urea index ([urea]/[amino acids]), normalizing plasma urea levels to plasma levels of total amino acids. In mice treated with GCGA, the urea index was increased 1.4-fold after four weeks of treatment compared to baseline (Figure 1I, p = 0.055), whereas the urea index remained the same in mice treated with PBS (Figure 1I, p = 0.5). In GCGR Ab-treated mice, the urea index was decreased by 61% at week four compared to baseline (Figure 1J, p < 0.0001) and did not change in Ctl Ab-treated mice (Figure 1J, p = 0.3). Collectively, these results support that the chronic enhancement of glucagon receptor signaling increases substrate-driven ureagenesis and lowers circulating amino acids, while chronic reduction of glucagon receptor signaling impairs amino acid metabolism as reflected by decreased ureagenesis, resulting in hyperaminoacidemia.

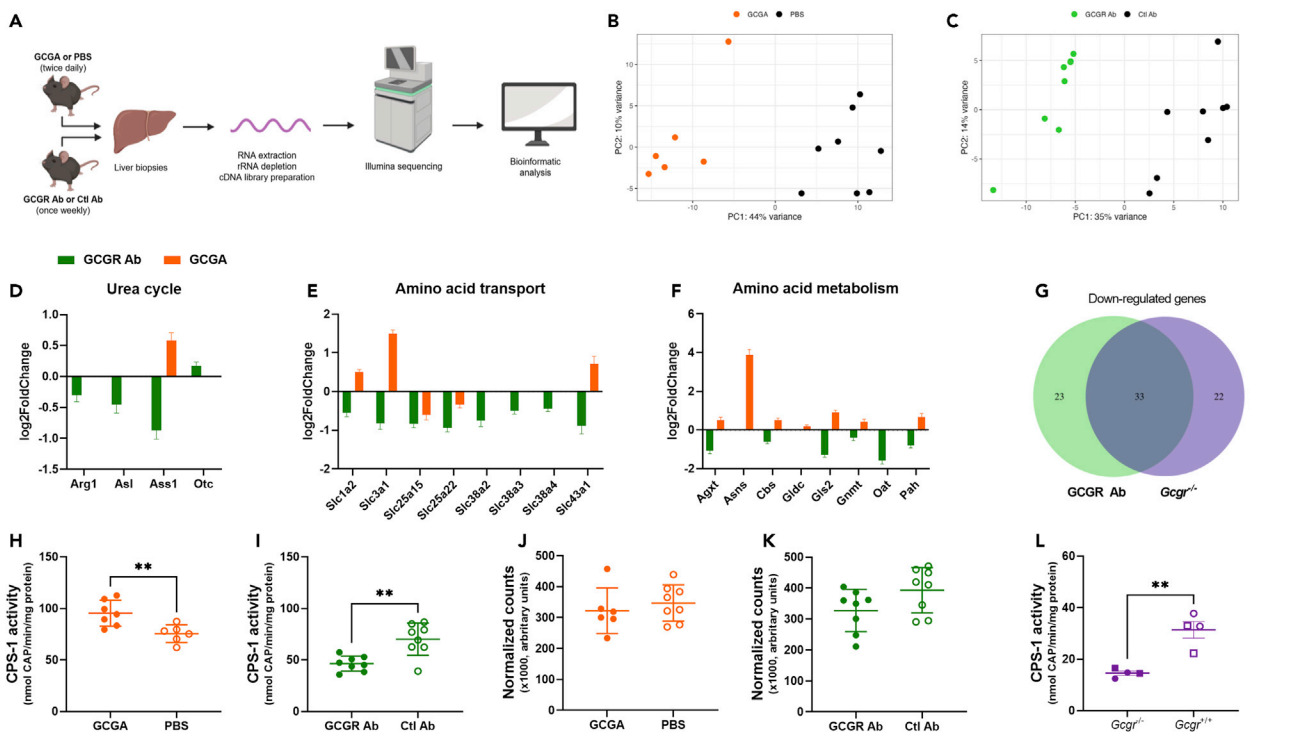

Figure 2. Chronic activation or inhibition of glucagon receptor signaling changes hepatic expression of amino acid metabolism and ureagenesis genes in opposite directions and regulates CPS-1 activity in female mice

(A) Workflow of RNA sequencing of liver biopsies from female C57BL/6JRj mice treated twice daily for eight weeks with a long-acting glucagon analog (GCGA, NNC9204-0043, 1.5 nmol/kg body weight) or PBS +1% BSA (PBS) or treated once weekly for eight weeks with a glucagon receptor antibody (GCGR Ab, REGN1193, Regeneron, 10 mg/kg body weight) or control antibody (Ctl Ab, REGN1945, Regeneron, 10 mg/kg body weight) (all mice seven weeks of age at the beginning of the study).

(B and C) Principal component analysis (PCA) of RNA sequencing samples from (B) GCGA- or PBS-treated mice or (C) GCGR Ab- or Ctl Ab-treated mice.

(D–F) Log2foldchanges of selected genes associated with (D) urea cycle, (E) amino acid transport, and (F) amino acid metabolism in the livers of mice treated for eight weeks with GCGA or GCGR Ab compared to their respective control groups (PBS or Ctl Ab). Only genes that were differentially expressed by FDR<0.05 are shown, thus when no bars are shown for GCGA (orange) or GCGR Ab (green) it means that the gene was not significantly differentially expressed when compared to the respective control groups (PBS or Ctl Ab). A detailed table of differentially expressed genes of interest is available in Table S2.

(G) Venn diagram showing the number of significantly down-regulated genes related to amino acid processes in GCGR Ab mice (green) and male *Gcgr*$^{-/-}$ mice (purple) from (Winther-Sorensen et al., 2020). The genes were selected using the Gene Ontology Biological Pathways (GOBP) umbrella terms "Cellular amino acid metabolic process," "Amino acid transport," "Amino acid homeostasis," and "Response to amino acid," and all related child terms. A table of genes included in this Venn Diagram is available in Table S3.

(H, I, and L) Enzymatic activity of carbamoyl phosphate synthetase-1 (CPS-1) in liver biopsies from female mice treated for eight weeks with (H) GCGA or PBS or (I) GCGR Ab or Ctl Ab; or in (L) *Gcgr*$^{-/-}$ and *Gcgr*$^{+/+}$ mice (10–11 weeks of age, females are circles, and males are squares).

(J and K) RNA sequencing data (DESeq2 normalized counts) of expression of Cps-1 in female mice treated with (J) GCGA or PBS or (K) GCGR Ab or Ctl Ab.

Data in (D-F) presented as mean ± SEM and (H–L) presented as mean ± SD, n = 4–8. FDR<0.05 was applied to all RNA sequencing analyses to correct for multiple testing, p-values in (H and I) by unpaired t-tests, *p < 0.05, **p < 0.01, ***p < 0.001, ****p < 0.0001.

Chronic alterations in glucagon receptor signaling in female mice affect plasma levels of all measured amino acids, but to different degrees

Given the observed changes in blood glucose levels, we hypothesized that treatment with GCGA and GCGR Ab would primarily affect the metabolism of the amino acids that can be used in gluconeogenesis, perhaps with particular effect on alanine and glutamine. We therefore measured the plasma levels of individual amino acids and calculated the fold change in amino acid levels from baseline to week four. Mice treated for four weeks with GCGA had decreased plasma levels of all 18 measured amino acids (Figure 1K) and the opposite were the case for mice treated with GCGR Ab (Figure 1L) (absolute plasma levels of the individual amino acid are available in Table S1). Thus, chronically increasing or decreasing glucagon receptor signaling affects the metabolism of all measured amino acids, suggesting the mechanism may involve a general regulation of amino acid metabolism, e.g. urea cycle flux.

Chronic activation or inhibition of glucagon receptor signaling in female mice changes the hepatic expression of amino acid metabolism and ureagenesis genes in opposite directions

To dissect the molecular mechanism underlying the observed effects on amino acid catabolism, we performed RNA sequencing of liver biopsies from female mice treated for eight weeks with GCGA or PBS, or with GCGR Ab or Ctl Ab (Figure 2A). Global gene expression profiles of the treatment groups (GCGA versus PBS and GCGR Ab versus Ctl Ab) were evaluated by principal component analysis (PCA) thereby reducing the multidimensional dataset into two dimensions. When projecting the data onto their first two principal components (PCs), the GCGA-treated mice clustered together and separately from PBS-treated mice (Figure 2B). Similarly, GCGR Ab-treated mice were clustered apart from Ctl Ab-treated mice (Figure 2C). Thus, the overall hepatic transcriptional profiles of the two treatment groups differed markedly from their control counterparts. 2,552 genes (of 18,750) were differentially expressed in GCGA-treated mice compared to PBS-treated mice (1,215 up-regulated and 1,337 down-regulated), and 1,813 genes (of 18,713) were differentially expressed in GCGR Ab-treated mice compared to Ctl Ab-treated mice (927 up-regulated and 886 down-regulated). To enable analysis and study of genes of interest, we developed two browsable apps, with which data on all the genes analyzed for differential expression can be found, visualized, and downloaded. These apps are publicly available at: https://weweralbrechtsenlab.shinyapps.io/GCGA/ and https://weweralbrechtsenlab.shinyapps.io/GCGR_Ab/. We searched for genes known to be associated with amino acid processes, and found genes related to the urea cycle (Figure 2D), amino acid transport (Figure 2E), and amino acid metabolism (Figure 2F) to be affected by altered glucagon receptor signaling (a list of genes of interest is available in Table S2). The urea cycle enzyme gene *Ass1* was up-regulated in GCGA-treated mice and down-regulated in GCGR Ab-treated mice. *Ass1* encodes the enzyme argininosuccinate synthetase, which catalyzes the third step of urea cycle, formation of argininosuccinate from citrulline and aspartate. Three of the four other genes encoding urea cycle enzymes (*Arg1*, *Asl*, and *Otc*) were also differentially expressed in the livers of GCGR Ab-treated mice (*Arg1* and *Asl* down-regulated, and *Otc* up-regulated) (Figure 2D). Mitochondrial transporters (*Slc25a15* and *Slc25a22*) were down-regulated in *both* GCGA- and GCGR Ab-treated mice. Slc25a15 is an ornithine carrier, transporting ornithine into the mitochondrial matrix and is essential for the urea cycle (Kunji et al., 2020). Slc25a22 facilitates mitochondrial glutamate import. In the mitochondria, glutamate may enter the tricarboxylic acid cycle, serve as a nitrogen source, or as a precursor to *N*-acetylglutamate (NAG) which is an activator of the urea cycle enzyme carbamoyl phosphate synthetase-1 (CPS-1) (Hensgens et al., 1980). The cytoplasmic amino acid transporters were up-regulated in GCGA-treated mice and down-regulated in GCGR Ab-treated mice (Figure 2E), e.g. Slc43a1, carrier of branched chain amino acids, and Slc1a2, a glutamic acid and aspartic acid transporter (Kandasamy et al., 2018). In addition, genes encoding enzymes involved in amino acid metabolism (general or specific for individual amino acids) were also up-regulated in the livers of GCGA-treated mice and down-regulated in the livers of GCGR Ab-treated mice (Figure 2F). The expression of *Gls2*, the gene encoding the liver isoform of glutaminase (Gls2), an enzyme delivering ammonia to the urea cycle (Meijer, 1985), was increased with a fold change of 1.89 in GCGA-treated mice and decreased with a fold change of 0.41 in GCGR Ab-treated mice. Expression of the gene *Asns*, encoding asparagine synthetase, showed a 14-fold increase in GCGA-treated mice, corresponding to our observation that plasma levels of asparagine had changed the most in both GCGA- and GCGR Ab-treated mice after four weeks of treatment (Figures 1L and 1K). We did not find a significant change in expression of *Asns* in GCGR Ab-treated mice. We then compared the differentially expressed genes in our GCGR Ab-treated mice to differentially expressed genes of livers of male glucagon receptor knock-out ($Gcgr^{-/-}$) mice, by reanalyzing the raw sequencing data from a data set previously published (Winther-Sorensen et al., 2020) so it matched our bioinformatic processing to compare the data sets directly. We likewise developed an app with these results, available via https://weweralbrechtsenlab.shinyapps.io/GcgrKO/. A total of 87 genes were up-regulated in the livers of both GCGR Ab and $Gcgr^{-/-}$ mice and 147 genes were down-regulated in both groups. We used Gene Ontology Biological Processes (GOBP) (Ashburner et al., 2000; Gene Ontology Consortium, 2021) to filter the differentially expressed genes annotated to all *child* terms of the umbrella terms "Cellular amino acid metabolic process," "Amino acid transport," "Amino acid homeostasis," and "Response to amino acid," and found, respectively, 56 and 55 genes that were down-regulated in GCGR Ab and $Gcgr^{-/-}$ mice, and 33 of these genes were down-regulated in *both* GCGR Ab treated mice and $Gcgr^{-/-}$ mice (Figure 2G). Thus, close to 1/4 of the 147 genes down-regulated in both GCGR Ab and $Gcgr^{-/-}$ mice were related to amino acid metabolism, indicating that the disruption of glucagon receptor signaling, whether pharmacological or genetic, has a substantial regulatory effect on the expression of genes related to amino acid processes.

Chronic glucagon receptor activation and inhibition in female mice, respectively, increases and decreases the enzymatic activity of carbamoyl phosphate synthethase-1

Hypothesizing that glucagon may increase ureagenesis also by non-transcriptional changes, we measured enzymatic activity of CPS-1 (the first and rate-limiting enzyme in hepatic ureagenesis) in liver biopsies from female mice with chronically increased or decreased glucagon receptor signaling. Treatment with GCGA increased CPS-1 activity compared to mice treated with PBS (Figure 2H, $p = 0.007$), while treatment with GCGR Ab decreased hepatic CPS-1 activity compared to mice treated with Ctl Ab (Figure 2I, $p = 0.002$). There was no difference in *Cps-1* expression in the RNA sequencing of the livers between GCGA- and PBS-treated mice (Figure 2J, adjusted p-value = 0.7) nor between GCGR Ab- and Ctl Ab-treated mice (Figure 2K, adjusted p-value = 0.2), indicating that glucagon regulates this first and rate-limiting step in ureagenesis through non-transcriptional mechanisms. We also measured CPS-1 activity in the livers of non-fasted $Gcgr^{-/-}$ mice and $Gcgr^{+/+}$ littermates. As seen in the livers of mice with pharmacological disruption of glucagon receptor signaling, $Gcgr^{-/-}$ mice had decreased CPS-1 activity (Figure 2L), further supporting the hypothesis, that non-transcriptional regulation of CPS-1 activity may be important in glucagon's regulation of the urea cycle.

Chronic activation or inhibition of glucagon receptor signaling in female mice *reduces and increases pancreatic glucagon content, respectively*

Having investigated how glucagon signaling affects amino acid metabolism in the liver, we now looked at how this might affect the pancreatic islets. Impaired amino acid metabolism has previously been shown to stimulate alpha cell proliferation (Solloway et al., 2015; Dean et al., 2017; Kim et al., 2017). We evaluated morphometric changes of the pancreases in female mice treated for eight weeks with GCGA, GCGR Ab, or their respective control treatments. Mice treated for eight weeks with GCGA had lower pancreas weights compared to mice treated with PBS (Figure 3A, $p = 0.002$), while mice treated with GCGR Ab had higher pancreas weights compared to mice treated with Ctl Ab (Figure 3B, $p = 0.0009$). Pancreatic glucagon content was dramatically reduced in GCGA-treated mice versus PBS-treated mice (Figure 3C, $p < 0.0001$), and increased 5.9-fold in GCGR Ab-treated mice versus Ctl Ab-treated mice (Figure 3D, $p = 0.06$). No difference was observed in pancreatic insulin content in GCGA-treated mice (Figure 3E), but GCGR Ab-treated mice had lower pancreatic insulin compared to Ctl Ab-treated mice (Figure 3F, $p = 0.006$). To confirm these findings, we performed immunohistochemical staining for glucagon-, insulin-, and somatostatin-positive cells. In the pancreas of GCGA-treated mice, the islets had reduced amounts of glucagon-positive cells, and in two of the mice, it was not possible to identify any glucagon-positive islets (Figure 3G, compared to PBS in Figures 3H and S2A), indicating extensive hypoplasia of the alpha cells. In contrast, alpha cell hyperplasia was evident in GCGR Ab-treated mice, in which the islets were enlarged and showed confluence. Glucagon-positive cells were widely dispersed in the islets (Figure 3I), contrasting to the peripheral location seen in the islets of Ctl Ab-treated mice (Figure 3J). In GCGR Ab-treated mice, the glucagon-positive cells occupied on average 60% of the islets, compared to 13% in the Ctl Ab-treated mice (Figure S2B). There was no difference in islet composition of beta cells in GCGA-treated mice compared to PBS-treated mice (Figure S2C). In GCGR Ab-treated mice, insulin-positive cells were substantially reduced in number and confined to the center of the islets (Figure 3K), contrasting to Ctl Ab-treated mice, in which insulin-positive cells dominated the islets (Figure 3L). Thus, the alpha cell hyperplasia co-occurred with a loss of beta cells (Figure S2D), supporting our measurements of the pancreatic insulin content (Figure 3F). We did not find any differences in the abundance of somatostatin-positive cells (Figures S2E and S2F). GCGA-treated mice had increased plasma glucagon levels after four weeks (caused by the exogenously administered glucagon, also picked up by the glucagon assay) (Figure 3M, $p < 0.0001$), but had no change in plasma insulin levels (Figure 3N, $p = 0.4$). This was in line with the observation that the pancreatic insulin content was the same in GCGA and PBS-treated mice (Figure 3D). Reflecting the observed changes in islet composition, GCGR Ab-treated mice showed significant hyperglucagonemia with a 55-fold change from week zero (Figure 3O, $p < 0.0001$) and plasma insulin levels were reduced (Figure 3P, $p = 0.002$). To summarize, our results show that chronic glucagon receptor antagonism affects the pancreatic islet composition of alpha and beta cells, while chronic glucagon receptor agonism seems to exclusively and extensively reduce pancreatic glucagon content.

DISCUSSION

We here studied hepatic amino acid metabolism and pancreatic islet integrity upon chronic glucagon receptor agonism and antagonism. Chronic glucagon receptor agonism (GCGA treatment) caused alpha cell hypoplasia, reduced plasma amino acid levels, increased substrate-induced ureagenesis (estimated by the

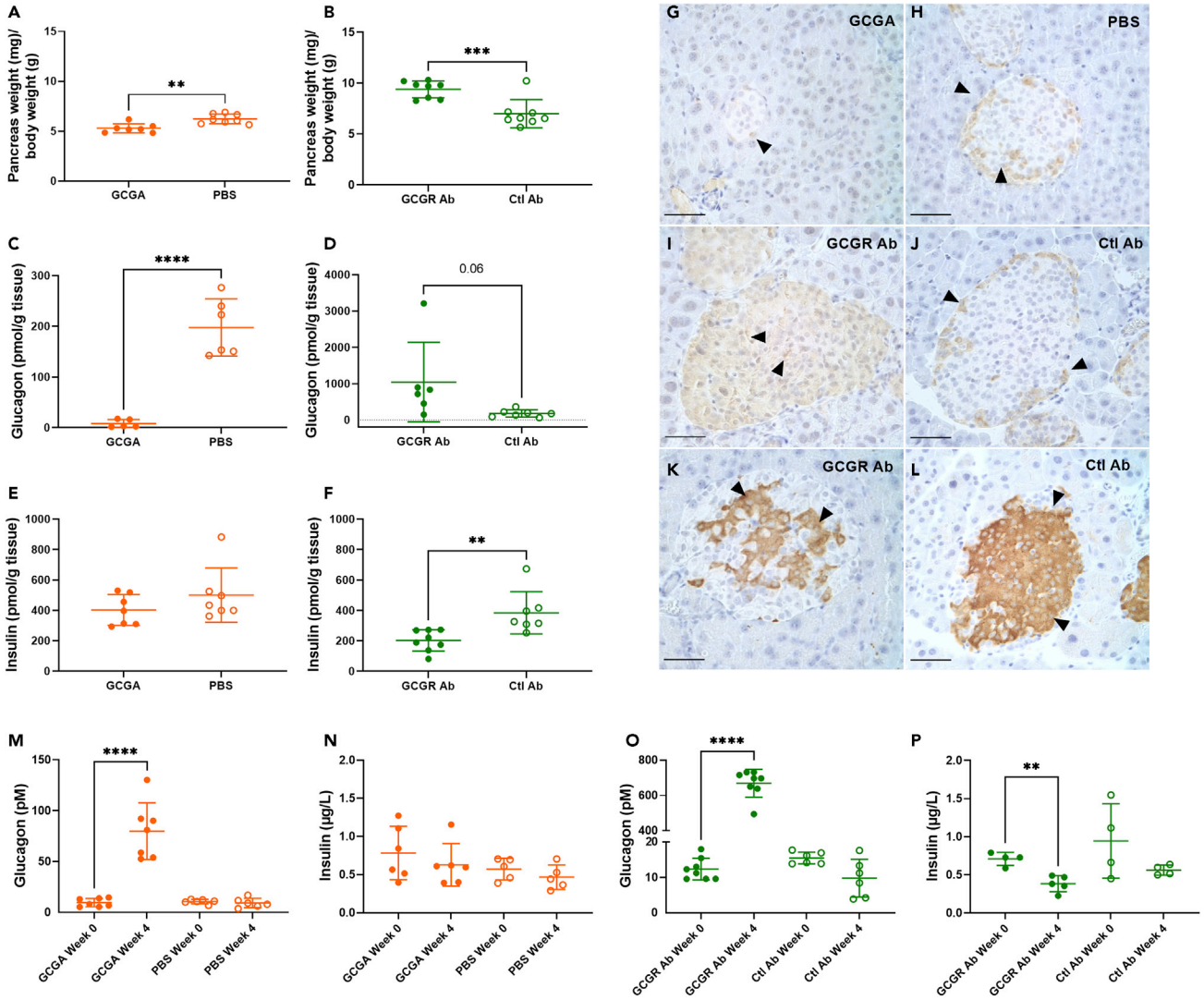

Figure 3. Chronic activation and inactivation of glucagon receptor signaling, respectively, reduce and increase pancreatic glucagon content in female mice

(A and B) Pancreas weights from female C57BL/6JRj mice treated (A) twice daily for eight weeks with a long-acting glucagon analog (GCGA, NNC9204-0043, 1.5 nmol/kg body weight) or PBS +1% BSA (PBS) or (B) treated once weekly for eight weeks with a glucagon receptor antibody (GCGR Ab, REGN1193, Regeneron, 10 mg/kg body weight) or control antibody (Ctl Ab, REGN1945, Regeneron, 10 mg/kg, body weight).

(C and D, NB! the y axes differ) Pancreatic glucagon and (E and F) insulin content in mice treated for eight weeks with (C and E) GCGA or PBS or (D and F) GCGR Ab or Ctl Ab.

(G–J) Immunohistochemical staining for glucagon-positive cells in the pancreases of mice treated with (G) GCGA, (H) PBS, (I) GCGR Ab, or (J) Ctl Ab.

(K and L) Immunohistochemical staining for insulin-positive cells in pancreases of mice treated with (K) GCGR Ab or (L) Ctl Ab. Black arrows indicate (G–J) glucagon- or (K and L) insulin-positive cells. Scale bar: 50 µm. See also Figure S2.

(M and O, NB! the y axes differ) Plasma glucagon levels in mice treated for four weeks with (M) GCGA or PBS or (O) GCGR Ab or Ctl Ab.

(N and P) Plasma insulin levels in mice treated for four weeks with (N) GCGA or PBS or (P) GCGR Ab or Ctl Ab. All blood samples were taken prior to injection. The mice were seven weeks of age at the beginning of the study. Data presented as mean ± SD, n = 4–8. p-values by unpaired t-tests, *$p < 0.05$, **$p < 0.01$, ***$p < 0.001$, ****$p < 0.0001$.

plasma urea index), and persistently increased blood glucose levels. Conversely, chronic glucagon receptor antagonism (GCGR Ab treatment) caused hyperaminoacidemia, hyperglucagonemia, alpha cell hyperplasia, and decreased the plasma urea index and blood glucose levels. We show that these changes are likely mediated by transcriptional changes in liver genes encoding proteins involved in amino acid metabolism, amino acid transport, and ureagenesis, and a non-transcriptional change in the enzymatic activity of the rate-limiting urea cycle enzyme CPS-1. Importantly, tying hepatic, plasma, and pancreatic changes

together, while providing molecular insight into how chronic glucagon excess also causes substantial hepatic and pancreatic changes, we show that both chronic activation and inhibition of glucagon receptor signaling result in pronounced changes in the liver-alpha cell axis (Richter et al., 2022), thus furthering our understanding of this axis.

Plasma levels of total amino acids were decreased in GCGA-treated mice and increased in GCGR Ab-treated mice. One unanswered question regarding the liver-alpha cell axis is to what extent the individual amino acids are involved in the liver-alpha cell axis, and which are affected, when the axis is disrupted or glucagon signaling is enhanced. We previously found alanine, arginine, cysteine, and proline to be involved in the acute regulation of the liver-alpha cell axis, as they increased glucagon secretion and their disappearance rate was altered by the inhibition of glucagon receptor signaling (Galsgaard et al., 2020a). We here investigated the liver-alpha cell upon chronic alterations of glucagon receptor signaling and found that plasma levels of all the 18 measured amino acids were decreased in GCGA-treated mice and increased in GCGR Ab-treated mice. Moreover, those amino acids that were changed the most (asparagine, threonine, alanine, methionine, and arginine) and least (leucine, isoleucine, glutamic acid, tryptophan, and phenylalanine) were generally the same in GCGA- and GCGR Ab-treated mice, and importantly alanine, arginine and proline, which acutely regulates the liver-alpha cell axis (Galsgaard et al., 2020a), were found among the nine most changed amino acids in both groups. The amino acid, asparagine, changed the most in both GCGA and GCGR Ab mice, and our RNA sequencing revealed a 14-fold increased expression of the gene encoding asparagine synthetase (*Asns*) in livers of GCGA-treated mice, which could be owing to the large reduction in plasma levels of asparagine. *Asns* was not, however, differentially expressed in GCGR Ab-treated mice, further indicating that more research into these mechanisms, and their potential relevance for the liver-alpha cell axis, is needed. In a previous study of *Gcgr*$^{-/-}$ mice, serum concentrations of methionine, threonine, and asparagine were also among the most up-regulated amino acids, whereas the branched chain and aromatic amino acids showed only minor or no changes (Solloway et al., 2015). The same pattern was observed in patients with NAFLD showing hyperglucagonemia and hyperaminoacidemia (Wewer Albrechtsen et al., 2018). Pancreatectomized subjects also show hyperaminoacidemia with increased plasma levels of alanine, arginine, citrulline, glycine, serine, threonine, and tyrosine (Boden et al., 1980), and conversely subjects with glucagon producing tumors (glucagonomas) show hypoaminoacidemia including decreased levels of the mentioned amino acids (except threonine which was not measured in the cited study) (Mallinson et al., 1974). Thus, it seems that the metabolism of branched-chain amino acids may be less affected by changes in glucagon receptor signaling compared to that of the remaining amino acids, and these amino acids may not be the main mediators of the liver-alpha cell axis. In particular alanine and glutamine have been suggested to play important roles in the liver-alpha cell axis, with alanine known to accelerate gluconeogenesis (Chiasson et al., 1975) and stimulate glucagon secretion (Galsgaard et al., 2020a), whereas glutamine may be essential for alpha cell proliferation (Dean et al., 2017), but not secretion as we previously found that glutamine did not stimulate glucagon secretion from the perfused mouse pancreas (Galsgaard et al., 2020a) and other studies using perifused islets found that glutamine stimulated glucagon secretion less potently than glycine and alanine (El et al., 2021; Capozzi et al., 2019). This may suggest that different mechanisms (i.e., amino acids) account for the alpha cell hyperplasia and the hyperglucagonemia observed in mice with disrupted glucagon receptor signaling. In our study, mice treated with GCGR Ab had a 3-fold increase in plasma levels of glutamine after four weeks of treatment, likely contributing to the morphometric changes in the pancreas. Mice treated with GCGR Ab had reduced pancreatic insulin content, and it could be speculated that this loss of beta cells may in part be caused by beta cells transdifferentiating into alpha cells, a process that has been demonstrated to occur *in vitro* (Spijker et al., 2013). GCGR Ab treatment has previously been shown to decrease blood glucose levels, to increase plasma levels of GLP-1, glucagon and amino acids and to cause alpha cell hyperplasia (Okamoto et al., 2015). Importantly, both the hyperglucagonemia and alpha cell hyperplasia were found to be reversible (Okamoto et al., 2015), and reversibility was also shown after treatment with a different glucagon receptor antibody (Gu et al., 2009; Watanabe et al., 2012). It may be speculated that the observed reversibility of hyperglucagonemia and alpha cell hyperplasia depend on the normalization of plasma amino acid concentrations, and similarly that the alpha cell hypoplasia upon GCGA treatment could potentially be reversible if plasma amino acids were raised to normal physiological levels.

One of the drivers of increased (GCGA) or decreased (GCGR Ab) amino acid metabolism seems to be changes in hepatic gene expression. RNA sequencing revealed that many genes related to amino acid metabolism were up-regulated in GCGA-treated mice and down-regulated in GCGR Ab-treated mice.

Comparing the transcriptional profile of GCGR Ab-treated mice to those obtained from livers of *Gcgr*$^{-/-}$ mice (Winther-Sorensen et al., 2020), we found 234 genes that were up- or down-regulated by both genetic and pharmacological disruption of glucagon receptor signaling. In contrast, in another study where mice were treated with a different GCGR antibody there were 658 genes overlapping with *Gcgr*$^{-/-}$ mice (Dean et al., 2017). The reason for this divergence may be that our GCGR Ab- and Ctl Ab-treated mice were fasted overnight (11 h) before the isolation of the livers, whereas the *Gcgr*$^{-/-}$ mice were only fasted for four hours. Thus, it is likely, that the transcriptome profiles may differ owing to different stages of fasting. Nevertheless, this limitation of our study was associated with an important observation: out of the 147 down-regulated genes overlapping between GCGR Ab and *Gcgr*$^{-/-}$ mice, 33 were annotated to amino acid related processes, suggesting that the effect of disrupting or inhibiting the glucagon receptor on the transcription of genes involved in amino acid metabolism is to some degree independent on the fasted/fed state. Several amino acid transporters (*Slc43a1*, *Slc1a2*, and *Slc3a1*) and amino acid metabolism genes (*Gls2*, *Pah*, *Agxt*, *Gnmt*, *Nnmt*, and *Cbs*) were differentially expressed in the two treatment groups and were also down-regulated in *Gcgr*$^{-/-}$ mice. Surprisingly, only the gene encoding the urea cycle enzyme argininosuccinate synthetase 1 (*Ass1*), was up-regulated in GCGA-treated mice, while in GCGR Ab-treated mice, the expression of four out of the five urea cycle genes was differentially expressed, all of which were down-regulated in *Gcgr*$^{-/-}$ mice. *Ass1* was also the most down-regulated urea cycle enzyme in a study with a different glucagon receptor antibody (Kim et al., 2017) and mice deprived of proglucagon (by the deletion of *Gcg*) showed decreased expression of *Ass1* (and several other amino acid metabolism genes) associated with hyperaminoacidemia (Watanabe et al., 2012). *Ass1* was also up -regulated in dairy cows treated with glucagon (Bobe et al., 2009), supporting a particularly important regulatory role for this enzyme.

Apart from looking at the transcriptional changes associated with increased or decreased glucagon receptor signaling, we measured the enzymatic activity of the ureagenesis enzyme CPS-1. CPS-1 is localized in the mitochondria of hepatocytes and is the first and rate-limiting enzyme in hepatic ureagenesis, catalyzing the conversion of bicarbonate and ammonium to carbamoyl phosphate (Thoden et al., 1999). Hepatic expression of *Cps-1* is increased by glucagon (Bobe et al., 2009; Kraft et al., 2017) and reduced by pharmacological (Kim et al., 2017) or genetic (Winther-Sorensen et al., 2020) disruption of the glucagon receptor. We found increased enzymatic activity of CPS-1 in GCGA-treated mice and decreased activity in GCGR Ab-treated mice, but we did not detect transcriptional differences in *Cps-1* expression between our treatment groups. *Gcgr*$^{-/-}$ mice also had decreased activity of CPS-1, further supporting that glucagon regulates the activity of this enzyme. In line with this, glucagon was proposed to increase ureagenesis by increasing CPS-1 activity *in vitro* (Snodgrass et al., 1978). This study reported increased activity of all five urea cycle enzymes (CPS-1, ornithine transcarbamylase, Ass1, arginosuccinate lyase, and arginase) in rat livers treated with crystalline zinc glucagon (in astronomical doses) (Snodgrass et al., 1978). A more recent study showed that glucagon activates sirtuin 3 and 5 that deacetylate and activate CPS-1 and ornithine transcarbamylase (Li et al., 2016). However, newer studies elucidating the liver-alpha cell axis have not covered this aspect, focusing instead on transcriptional changes (Solloway et al., 2015; Kim et al., 2017; Dean et al., 2017; Winther-Sorensen et al., 2020). Our study suggests that the increased activity of CPS-1 may be owing to a non-transcriptional regulation of the enzyme by glucagon. Glucagon increases the mitochondrial concentrations of the allosteric CPS-1 co-factor NAG (Hensgens et al., 1980). We did not find transcriptional differences in the gene encoding *N*-acetylglutamate synthase (*Nags*), which catalyzes the production of NAG, but this does not rule out the possibility that this enzyme conveys the glucagon-stimulated increase in CPS-1 activity. The enzyme Gls2 could also be involved in this regulation. Gls2 deaminates glutamine to form glutamate and ammonia, which are substrates for NAGS and CPS-1, respectively (Meijer, 1985; Brosnan et al., 1995; Nissim et al., 1999) and glucagon may increase this deamination. Glucagon has been shown to increase glutaminolysis ~3-fold in primary mouse hepatocytes, resulting in a shift from lactate to glutamine as the glucogenic substrate (Miller et al., 2018), and RNA and protein levels of Gls2 decreased in another study of high protein fed mice treated for 39 days with the same antibody as the one used in this study (GCGR Ab) (Cavino et al., 2021). In line with this, we found increased expression of *Gls2* in the livers of GCGA-treated mice and decreased expression in GCGR Ab-treated mice. Thus, it seems there could be multiple routes for or contributions to modulating CPS-1 activity, and how glucagon specifically is involved is obviously of great interest.

The hyperglycemic effect of excess glucagon and the reports of hyperglucagonemia in patients with type 2 diabetes (Raskin and Unger, 1978; Reaven et al., 1987; Faerch et al., 2016) and NAFLD (Junker et al., 2016; Wewer Albrechtsen et al., 2018; Suppli et al., 2020) have led to the development of glucagon receptor

antagonists to lower blood glucose levels in these patients. The compounds were successful in reducing blood glucose and HbA_{1C} levels, but the therapy is associated with small but consistent elevations in serum amino transferases (Kazda et al., 2016; Kostic et al., 2018; Kazierad et al., 2018) (clinically used as a marker of liver inflammation), and accumulation of hepatic fat and increased plasma cholesterol (Guzman et al., 2017). However, to our knowledge, no study reported amino acid or urea levels in the patients. We here show that these parameters should be addressed, as hyperaminoacidemia may result from treatment with these compounds. Another newer treatment focus has been on dual agonists of the glucagon receptor (expected to increase energy expenditure and decrease appetite) and of the GLP-1 receptor (suppressing food intake and enhancing insulin secretion) (Henderson et al., 2016; Ambery et al., 2018; Tillner et al., 2019). The clinically relevant parameters, body weight, and food intake, were improved by these dual agonists (Tillner et al., 2019; Ambery et al., 2018; Pocai et al., 2009; Day et al., 2009), and chronic glucagon receptor activation, using a long-acting agonist, also resulted in weight loss and decreased food intake (Habegger et al., 2013; Kim et al., 2018; Nason et al., 2021). In line with these findings, we observed a decrease in body weight upon GCGA treatment and an increase upon GCGR Ab treatment following the eight weeks of treatment. However, a study in rodents and monkeys emphasized the importance of measuring amino acid parameters, as a glucagon/GLP-1 receptor dual agonist decreased plasma amino acids and increased hepatic expression of amino acid transporters (Li et al., 2020). Our study confirms that glucagon agonism potently accelerates amino acid metabolism, exposing a possible limitation in the use of these drugs. Indeed, a recent study in overweight or obese individuals identified plasma amino acids as the dominating metabolites separating groups infused for 23 h with glucagon from the group treated with placebo (Vega et al., 2021). This supports that amino acids may be viewed as particularly a sensitive biomarker for changes in glucagon receptor signaling. Our study also shows that chronic glucagon receptor agonism causes alpha cell hypoplasia which may add an additional limitation in the use of drugs agonizing the receptor. Thus, when interfering with glucagon receptor signaling, whether by antagonizing the receptor or increasing signaling, the liver-alpha cell axis must be addressed, and plasma amino acid levels and pancreatic islet integrity should be considered.

The extremely short half-life (~2 min) of native glucagon has previously made chronic *in vivo* experimental activation of glucagon receptor signaling difficult, particularly in rodents, but with GCGA, an acylated glucagon peptide, the half-life has been expanded from minutes (Wewer Albrechtsen et al., 2016b) to 5–6 h (subcutaneous injection, 3 nmol/kg body weight). Our dosage (1.5 nmol/kg body weight) was designed to provide therapeutically relevant plasma concentrations of glucagon (endogenous concentrations up to 100 pM) and allowed us to study the effects of chronic elevations in glucagon receptor signaling without genetic tampering, i.v. infusions, or repeated injections of pharmacological doses. Our protocol enabled us to not only corroborate previous findings (Gelling et al., 2003; Solloway et al., 2015) that the disruption of the glucagon receptor (GCGR Ab treatment) causes alpha cell hyperplasia, but we also show that chronically elevated glucagon receptor signaling caused a significant reduction in pancreatic glucagon content and alpha cell hypoplasia. This observation, which is in agreement with previous observations of alpha cell hypoplasia in rats (Blume et al., 1995) and mice (Drucker et al., 1992) with transplanted glucagon-producing tumors and in glucagon-treated rabbits (Lazarus and Volk, 1958; Logothetopoulos and Salter, 1960; Logothetopoulos et al., 1960), is another example of the extensive biological consequences of increased glucagon receptor signaling. The alpha cells seemed to recover to their normal appearance extremely slowly after the glucagon treatment (Logothetopoulos et al., 1960), suggesting that, like the alpha cell hyperplasia observed upon disrupted glucagon receptor signaling, the observed alpha cell hypoplasia may also be reversible. This study provides a comprehensive evaluation of the physiological effects of interfering with the integrity of liver-alpha cell axis, showing that the axis is a tightly regulated feedback system that is sensitive to perturbations in either direction of glucagon receptor signaling. The study provides insight into transcriptional and non-transcriptional mechanisms underpinning the liver part of the axis, highlighting CPS-1 activity as a possible key component of glucagon's regulation of ureagenesis. Based on our findings, we argue that investigating liver-alpha cell axis integrity is crucial when evaluating glucagon-based drugs, and our findings support the use of plasma amino acid levels as a marker of glucagon receptor signaling.

Limitations of the study

Only female mice were used to avoid potential injuries owing to fighting between male mice, potentially resulting in group reductions. For ethical reasons, we did not use single-housed male mice. Furthermore, we used female mice to allow comparisons with our previous findings regarding the liver-alpha cell axis (Galsgaard et al., 2018, 2019, 2020a, 2020b; Kjeldsen et al., 2021; Winther-Sorensen et al., 2020).

STAR★METHODS

Detailed methods are provided in the online version of this paper and include the following:

- KEY RESOURCES TABLE
- RESOURCE AVAILABILITY
  - Lead contact
  - Materials availability
  - Data and code availability
- EXPERIMENTAL MODEL AND SUBJECT DETAILS
  - Animals
  - Treatment
- METHOD DETAILS
  - Preparation of the long-acting glucagon analog, GCGA, NNC9204-0043
  - Biochemical analyses
  - Histology
  - Plasma amino acid quantitation via liquid chromatography-mass spectrometry
  - RNA sequencing
  - Bioinformatic analysis of RNA sequencing data
- QUANTIFICATION AND STATISTICAL ANALYSIS

SUPPLEMENTAL INFORMATION

Supplemental information can be found online at https://doi.org/10.1016/j.isci.2022.105296.

ACKNOWLEDGMENTS

We thank Regeneron for providing the antibodies REGN1193 and REGN1945. We thank Maureen J. Charron, Departments of Biochemistry, Obstetrics and Gynecology and Women's Health, and Medicine, Albert Einstein College of Medicine, New York, for providing glucagon receptor knockout mice. We thank the Center for Genomic Medicine, Rigshospitalet, Denmark for performing RNA sequencing. We thank laboratory technician Heidi Marie Paulsen for the preparation and staining of pancreas slices and Associate Professor Jens Brings Jacobsen for access to his microscope. This work was supported by the Novo Nordisk Foundation (NNF) Center for Basic Metabolic Research University of Copenhagen, (NNF Application Number: 13563); NNF Project Support in Endocrinology and Metabolism-Nordic Region (NNF Application Number: 34250). Emilie Elmelund is supported by the Novo Scholarship Program (2022). Nicolai J. Wewer Albrechtsen is supported by an NNF Excellence Emerging Investigator Grant – Endocrinology and Metabolism (NNF19OC0055001), EFSD Future Leader Award (NNF21SA0072746) and Independent Research Fund, Sapere Aude (1052-00003B). Novo Nordisk Foundation Center for Protein Research is supported by the Novo Nordisk Foundation (grant agreement NNF14CC0001). The data were presented at American Diabetes Association's 82nd Scientific Session, June 3rd -7th, New Orleans, LA, USA. The graphical abstract is created with BioRender.com.

AUTHOR CONTRIBUTIONS

Conceptualization, K.D.G., J.J.H., N.J.W.A.; resources, T.K., J.F.L.; investigation, E.E., K.D.G., A.B.B., J.E.H., S.A.J.T.; formal analysis, E.E., K.D.G., C.D.J.; visualization, E.E., K.D.G., C.D.J.; writing – original draft, E.E.; writing – review & editing, K.D.G., C.D.J., S.A.J.T., A.B.B., M.W.S., J.E.H., C.M.S., T.K., J.F.L, T.J.G., J.J.H., N.J.W.A.; supervision and funding acquisition, J.J.H., N.J.W.A. All authors approved the final version of the article.

DECLARATION OF INTERESTS

Thomas Kruse and Jesper F. Lau are employed by Novo Nordisk A/S. No conflicts of interest, financial or otherwise, are declared by the remaining authors.

Received: July 21, 2022
Revised: August 29, 2022
Accepted: September 30, 2022
Published: November 18, 2022

REFERENCES

Ambery, P., Parker, V.E., Stumvoll, M., Posch, M.G., Heise, T., Plum-Moerschel, L., Tsai, L.F., Robertson, D., Jain, M., Petrone, M., et al. (2018). MEDI0382, a GLP-1 and glucagon receptor dual agonist, in obese or overweight patients with type 2 diabetes: a randomised, controlled, double-blind, ascending dose and phase 2a study. Lancet *391*, 2607–2618. https://doi.org/10.1016/S0140-6736(18)30726-8.

Anders, S., and Huber, W. (2010). Differential expression analysis for sequence count data. Genome Biol. *11*, R106. https://doi.org/10.1186/gb-2010-11-10-r106.

Ashburner, M., Ball, C.A., Blake, J.A., Botstein, D., Butler, H., Cherry, J.M., Davis, A.P., Dolinski, K., Dwight, S.S., Eppig, J.T., et al. (2000). Gene ontology: tool for the unification of biology. The Gene Ontology Consortium. Nat. Genet. *25*, 25–29. https://doi.org/10.1038/75556.

Blume, N., Skouv, J., Larsson, L.I., Holst, J.J., and Madsen, O.D. (1995). Potent inhibitory effects of transplantable rat glucagonomas and insulinomas on the respective endogenous islet cells are associated with pancreatic apoptosis. J. Clin. Invest. *96*, 2227–2235. https://doi.org/10.1172/JCI118278.

Bobe, G., Velez, J.C., Beitz, D.C., and Donkin, S.S. (2009). Glucagon increases hepatic mRNA concentrations of ureagenic and gluconeogenic enzymes in early-lactation dairy cows. J. Dairy Sci. *92*, 5092–5099. https://doi.org/10.3168/jds.2009-2152.

Boden, G., Master, R.W., Rezvani, I., Palmer, J.P., Lobe, T.E., and Owen, O.E. (1980). Glucagon deficiency and hyperaminoacidemia after total pancreatectomy. J. Clin. Invest. *65*, 706–716. https://doi.org/10.1172/jci109717.

Brosnan, J.T., Ewart, H.S., and Squires, S.A. (1995). Hormonal control of hepatic glutaminase. Adv. Enzym. Regul. *35*, 131–146. https://doi.org/10.1016/0065-2571(94)00003-l.

Capozzi, M.E., Wait, J.B., Koech, J., Gordon, A.N., Coch, R.W., Svendsen, B., Finan, B., D'alessio, D.A., and Campbell, J.E. (2019). Glucagon lowers glycemia when beta-cells are active. JCI Insight *5*, e129954. https://doi.org/10.1172/jci.insight.129954.

Carlson, M. (2022). GO.db: a set of annotation maps describing the entire Gene Ontology. R package version 3.8.2. https://doi.org/10.18129/B9.bioc.GO.db.

Cavino, K., Sung, B., Su, Q., Na, E., Kim, J., Cheng, X., Gromada, J., and Okamoto, H. (2021). Glucagon receptor inhibition reduces hyperammonemia and lethality in male mice with urea cycle disorder. Endocrinology *162*, bqaa211. https://doi.org/10.1210/endocr/bqaa211.

Chiasson, J.L., Liljenquist, J.E., Sinclair-Smith, B.C., and Lacy, W.W. (1975). Gluconeogenesis from alanine in normal postabsorptive man. Intrahepatic stimulatory effect of glucagon. Diabetes *24*, 574–584. https://doi.org/10.2337/diab.24.6.574.

Day, J.W., Ottaway, N., Patterson, J.T., Gelfanov, V., Smiley, D., Gidda, J., Findeisen, H., Bruemmer, D., Drucker, D.J., Chaudhary, N., et al. (2009). A new glucagon and GLP-1 co-agonist eliminates obesity in rodents. Nat. Chem. Biol. *5*, 749–757. https://doi.org/10.1038/nchembio.209.

Dean, E.D., Li, M., Prasad, N., Wisniewski, S.N., Von Deylen, A., Spaeth, J., Maddison, L., Botros, A., Sedgeman, L.R., Bozadjieva, N., et al. (2017). Interrupted glucagon signaling reveals hepatic alpha cell Axis and role for L-glutamine in alpha cell proliferation. Cell Metabol. *25*, 1362–1373.e5. https://doi.org/10.1016/j.cmet.2017.05.011.

Drucker, D.J., Lee, Y.C., Asa, S.L., and Brubaker, P.L. (1992). Inhibition of pancreatic glucagon gene expression in mice bearing a subcutaneous glucagon-producing GLUTag transplantable tumor. Mol. Endocrinol. *6*, 2175–2184. https://doi.org/10.1210/mend.6.12.1491697.

El, K., Gray, S.M., Capozzi, M.E., Knuth, E.R., Jin, E., Svendsen, B., Clifford, A., Brown, J.L., Encisco, S.E., Chazotte, B.M., et al. (2021). GIP mediates the incretin effect and glucose tolerance by dual actions on alpha cells and beta cells. Sci. Adv. *7*, eabf1948. https://doi.org/10.1126/sciadv.abf1948.

Færch, K., Vistisen, D., Pacini, G., Torekov, S.S., Johansen, N.B., Witte, D.R., Jonsson, A., Pedersen, O., Hansen, T., Lauritzen, T., et al. (2016). Insulin resistance is accompanied by increased fasting glucagon and delayed glucagon suppression in individuals with normal and impaired glucose regulation. Diabetes *65*, 3473–3481. https://doi.org/10.2337/db16-0240.

Galsgaard, K.D., Jepsen, S.L., Kjeldsen, S.A.S., Pedersen, J., Wewer Albrechtsen, N.J., and Holst, J.J. (2020a). Alanine, arginine, cysteine, and proline, but not glutamine, are substrates for, and acute mediators of, the liver-alpha-cell axis in female mice. Am. J. Physiol. Endocrinol. Metab. *318*, E920–E929. https://doi.org/10.1152/ajpendo.00459.2019.

Galsgaard, K.D., Pedersen, J., Kjeldsen, S.A.S., Winther-Sørensen, M., Stojanovska, E., Vilstrup, H., Ørskov, C., Wewer Albrechtsen, N.J., and Holst, J.J. (2020b). Glucagon receptor signaling is not required for N-carbamoyl glutamate- and l-citrulline-induced ureagenesis in mice. Am. J. Physiol. Gastrointest. Liver Physiol. *318*, G912–G927. https://doi.org/10.1152/ajpgi.00294.2019.

Galsgaard, K.D., Winther-Sørensen, M., Ørskov, C., Kissow, H., Poulsen, S.S., Vilstrup, H., Prehn, C., Adamski, J., Jepsen, S.L., Hartmann, B., et al. (2018). Disruption of glucagon receptor signaling causes hyperaminoacidemia exposing a possible liver-alpha-cell axis. Am. J. Physiol. Endocrinol. Metab. *314*, E93–E103. https://doi.org/10.1152/ajpendo.00198.2017.

Galsgaard, K.D., Winther-Sørensen, M., Pedersen, J., Kjeldsen, S.A.S., Rosenkilde, M.M., Wewer Albrechtsen, N.J., and Holst, J.J. (2019). Glucose and amino acid metabolism in mice depend mutually on glucagon and insulin receptor signaling. Am. J. Physiol. Endocrinol. Metab. *316*, E660–E673. https://doi.org/10.1152/ajpendo.00410.2018.

Gelling, R.W., Du, X.Q., Dichmann, D.S., Romer, J., Huang, H., Cui, L., Obici, S., Tang, B., Holst, J.J., Fledelius, C., et al. (2003). Lower blood glucose, hyperglucagonemia, and pancreatic alpha cell hyperplasia in glucagon receptor knockout mice. Proc. Natl. Acad. Sci. USA *100*, 1438–1443. https://doi.org/10.1073/pnas.0237106100.

Gene Ontology Consortium (2021). The Gene Ontology resource: enriching a GOld mine. Nucleic Acids Res. *49*, D325–D334. https://doi.org/10.1093/nar/gkaa1113.

Gu, W., Yan, H., Winters, K.A., Komorowski, R., Vonderfecht, S., Atangan, L., Sivits, G., Hill, D., Yang, J., Bi, V., et al. (2009). Long-term inhibition of the glucagon receptor with a monoclonal antibody in mice causes sustained improvement in glycemic control, with reversible alpha-cell hyperplasia and hyperglucagonemia. J. Pharmacol. Exp. Ther. *331*, 871–881. https://doi.org/10.1124/jpet.109.157685.

Guzman, C.B., Zhang, X.M., Liu, R., Regev, A., Shankar, S., Garhyan, P., Pillai, S.G., Kazda, C., Chalasani, N., and Hardy, T.A. (2017). Treatment with LY2409021, a glucagon receptor antagonist, increases liver fat in patients with type 2 diabetes. Diabetes Obes. Metabol. *19*, 1521–1528. https://doi.org/10.1111/dom.12958.

Habegger, K.M., Heppner, K.M., Geary, N., Bartness, T.J., Dimarchi, R., and Tschöp, M.H. (2010). The metabolic actions of glucagon revisited. Nat. Rev. Endocrinol. *6*, 689–697. https://doi.org/10.1038/nrendo.2010.187.

Habegger, K.M., Stemmer, K., Cheng, C., Müller, T.D., Heppner, K.M., Ottaway, N., Holland, J., Hembree, J.L., Smiley, D., Gelfanov, V., et al. (2013). Fibroblast growth factor 21 mediates specific glucagon actions. Diabetes *62*, 1453–1463. https://doi.org/10.2337/db12-1116.

Henderson, S.J., Konkar, A., Hornigold, D.C., Trevaskis, J.L., Jackson, R., Fritsch Fredin, M., Jansson-Löfmark, R., Naylor, J., Rossi, A., Bednarek, M.A., et al. (2016). Robust anti-obesity and metabolic effects of a dual GLP-1/glucagon receptor peptide agonist in rodents and non-human primates. Diabetes Obes. Metabol. *18*, 1176–1190. https://doi.org/10.1111/dom.12735.

Hensgens, H.E., Verhoeven, A.J., and Meijer, A.J. (1980). The relationship between intramitochondrial N-acetylglutamate and activity of carbamoyl-phosphate synthetase (ammonia). The effect of glucagon. Eur. J. Biochem. *107*, 197–205. https://doi.org/10.1111/j.1432-1033.1980.tb04640.x.

Junker, A.E., Gluud, L., Holst, J.J., Knop, F.K., and Vilsbøll, T. (2016). Diabetic and nondiabetic patients with nonalcoholic fatty liver disease have an impaired incretin effect and fasting hyperglucagonaemia. J. Intern. Med. *279*, 485–493. https://doi.org/10.1111/joim.12462.

Kandasamy, P., Gyimesi, G., Kanai, Y., and Hediger, M.A. (2018). Amino acid transporters revisited: new views in health and disease. Trends Biochem. Sci. *43*, 752–789. https://doi.org/10.1016/j.tibs.2018.05.003.

Kazda, C.M., Ding, Y., Kelly, R.P., Garhyan, P., Shi, C., Lim, C.N., Fu, H., Watson, D.E., Lewin, A.J., Landschulz, W.H., et al. (2016). Evaluation of efficacy and safety of the glucagon receptor antagonist LY2409021 in patients with type 2 diabetes: 12- and 24-week phase 2 studies.

Diabetes Care *39*, 1241–1249. https://doi.org/10.2337/dc15-1643.

Kazierad, D.J., Chidsey, K., Somayaji, V.R., Bergman, A.J., and Calle, R.A. (2018). Efficacy and safety of the glucagon receptor antagonist PF-06291874: a 12-week, randomized, dose-response study in patients with type 2 diabetes mellitus on background metformin therapy. Diabetes Obes. Metabol. *20*, 2608–2616. https://doi.org/10.1111/dom.13440.

Kim, J., Okamoto, H., Huang, Z., Anguiano, G., Chen, S., Liu, Q., Cavino, K., Xin, Y., Na, E., Hamid, R., et al. (2017). Amino acid transporter Slc38a5 controls glucagon receptor inhibition-induced pancreatic alpha cell hyperplasia in mice. Cell Metabol. *25*, 1348–1361.e8. https://doi.org/10.1016/j.cmet.2017.05.006.

Kim, T., Nason, S., Holleman, C., Pepin, M., Wilson, L., Berryhill, T.F., Wende, A.R., Steele, C., Young, M.E., Barnes, S., et al. (2018). Glucagon receptor signaling regulates energy metabolism via hepatic farnesoid X receptor and fibroblast growth factor 21. Diabetes *67*, 1773–1782. https://doi.org/10.2337/db17-1502.

Kjeldsen, S.A.S., Hansen, L.H., Esser, N., Mongovin, S., Winther-Sørensen, M., Galsgaard, K.D., Hunt, J.E., Kissow, H., Ceutz, F.R., Terzic, D., et al. (2021). Neprilysin inhibition increases glucagon levels in humans and mice with potential effects on amino acid metabolism. J. Endocr. Soc. *5*, bvab084. https://doi.org/10.1210/jendso/bvab084.

Kostic, A., King, T.A., Yang, F., Chan, K.C., Yancopoulos, G.D., Gromada, J., and Harp, J.B. (2018). A first-in-human pharmacodynamic and pharmacokinetic study of a fully human anti-glucagon receptor monoclonal antibody in normal healthy volunteers. Diabetes Obes. Metabol. *20*, 283–291. https://doi.org/10.1111/dom.13075.

Kraft, G., Coate, K.C., Winnick, J.J., Dardevet, D., Donahue, E.P., Cherrington, A.D., Williams, P.E., and Moore, M.C. (2017). Glucagon's effect on liver protein metabolism in vivo. Am. J. Physiol. Endocrinol. Metab. *313*. E263–e272. https://doi.org/10.1152/ajpendo.00045.2017.

Kunji, E.R.S., King, M.S., Ruprecht, J.J., and Thangaratnarajah, C. (2020). The SLC25 carrier family: important transport proteins in mitochondrial physiology and pathology. Physiology *35*, 302–327. https://doi.org/10.1152/physiol.00009.2020.

Lau, J., Bloch, P., Schäffer, L., Pettersson, I., Spetzler, J., Kofoed, J., Madsen, K., Knudsen, L.B., Mcguire, J., Steensgaard, D.B., et al. (2015). Discovery of the once-weekly glucagon-like peptide-1 (GLP-1) analogue semaglutide. J. Med. Chem. *58*, 7370–7380. https://doi.org/10.1021/acs.jmedchem.5b00726.

Lazarus, S.S., and Volk, B.W. (1958). The effect of protracted glucagon administration on blood glucose and on pancreatic morphology. Endocrinology *63*, 359–371. https://doi.org/10.1210/endo-63-3-359.

Li, L., Zhang, P., Bao, Z., Wang, T., Liu, S., and Huang, F. (2016). PGC-1alpha promotes ureagenesis in mouse periportal hepatocytes through SIRT3 and SIRT5 in response to glucagon. Sci. Rep. *6*, 24156. https://doi.org/10.1038/srep24156.

Li, W., Kirchner, T., Ho, G., Bonilla, F., D'aquino, K., Littrell, J., Zhang, R., Jian, W., Qiu, X., Zheng, S., et al. (2020). Amino acids are sensitive glucagon receptor-specific biomarkers for glucagon-like peptide-1 receptor/glucagon receptor dual agonists. Diabetes Obes. Metabol. *22*, 2437–2450. https://doi.org/10.1111/dom.14173.

Liu, Z., Tu, M.J., Zhang, C., Jilek, J.L., Zhang, Q.Y., and Yu, A.M. (2019). A reliable LC-MS/MS method for the quantification of natural amino acids in mouse plasma: method validation and application to a study on amino acid dynamics during hepatocellular carcinoma progression. J. Chromatogr. B Analyt. Technol. Biomed. Life Sci. *1124*, 72–81. https://doi.org/10.1016/j.jchromb.2019.05.039.

Logothetopoulos, J., and Salter, J.M. (1960). Morphology and cytochemistry of alpha cells of the rabbit pancreas: effects of glucagon, insulin and infusions of glucose. Diabetes *9*, 31–37. https://doi.org/10.2337/diab.9.1.31.

Logothetopoulos, J., Sharma, B.B., Salter, J.M., and Best, C.H. (1960). Glucagon and metaglucagon diabetes in rabbits. Diabetes *9*, 278–285. https://doi.org/10.2337/diab.9.4.278.

Mallinson, C.N., Bloom, S.R., Warin, A.P., Salmon, P.R., and Cox, B. (1974). A glucagonoma syndrome. Lancet *2*, 1–5. https://doi.org/10.1016/s0140-6736(74)91343-9.

Meijer, A.J. (1985). Channeling of ammonia from glutaminase to carbamoyl-phosphate synthetase in liver mitochondria. FEBS Lett. *191*, 249–251. https://doi.org/10.1016/0014-5793(85)80018-1.

Miller, R.A., Shi, Y., Lu, W., Pirman, D.A., Jatkar, A., Blatnik, M., Wu, H., Cárdenas, C., Wan, M., Foskett, J.K., et al. (2018). Targeting hepatic glutaminase activity to ameliorate hyperglycemia. Nat. Med. *24*, 518–524. https://doi.org/10.1038/nm.4514.

Müller, T.D., Finan, B., Clemmensen, C., Dimarchi, R.D., and Tschöp, M.H. (2017). The new biology and pharmacology of glucagon. Physiol. Rev. *97*, 721–766. https://doi.org/10.1152/physrev.00025.2016.

Nason, S.R., Antipenko, J., Presedo, N., Cunningham, S.E., Pierre, T.H., Kim, T., Paul, J.R., Holleman, C., Young, M.E., Gamble, K.L., et al. (2021). Glucagon receptor signaling regulates weight loss via central KLB receptor complexes. JCI Insight *6*, e141323. https://doi.org/10.1172/jci.insight.141323.

Nissim, I., Brosnan, M.E., Yudkoff, M., and Brosnan, J.T. (1999). Studies of hepatic glutamine metabolism in the perfused rat liver with (15)N-labeled glutamine. J. Biol. Chem. *274*, 28958–28965. https://doi.org/10.1074/jbc.274.41.28958.

Noureddin, M., Ntanios, F., Malhotra, D., Hoover, K., Emir, B., Mcleod, E., and Alkhouri, N. (2022). Predicting NAFLD prevalence in the United States using National Health and Nutrition Examination Survey 2017-2018 transient elastography data and application of machine learning. Hepatol. Commun. *6*, 1537–1548. https://doi.org/10.1002/hep4.1935.

Okamoto, H., Kim, J., Aglione, J., Lee, J., Cavino, K., Na, E., Rafique, A., Kim, J.H., Harp, J., Valenzuela, D.M., et al. (2015). Glucagon receptor blockade with a human antibody normalizes blood glucose in diabetic mice and monkeys. Endocrinology *156*, 2781–2794. https://doi.org/10.1210/en.2015-1011.

Patro, R., Duggal, G., Love, M.I., Irizarry, R.A., and Kingsford, C. (2017). Salmon provides fast and bias-aware quantification of transcript expression. Nat. Methods *14*, 417–419. https://doi.org/10.1038/nmeth.4197.

Pearson, M.J., Unger, R.H., and Holland, W.L. (2016). Clinical trials, triumphs, and tribulations of glucagon receptor antagonists. Diabetes Care *39*, 1075–1077. https://doi.org/10.2337/dci15-0033.

Pierson, D.L. (1980). A rapid colorimetric assay for carbamyl phosphate synthetase I. J. Biochem. Biophys. Methods *3*, 31–37. https://doi.org/10.1016/0165-022x(80)90004-4.

Pocai, A., Carrington, P.E., Adams, J.R., Wright, M., Eiermann, G., Zhu, L., Du, X., Petrov, A., Lassman, M.E., Jiang, G., et al. (2009). Glucagon-like peptide 1/glucagon receptor dual agonism reverses obesity in mice. Diabetes *58*, 2258–2266. https://doi.org/10.2337/db09-0278.

Raskin, P., and Unger, R.H. (1978). Hyperglucagonemia and its suppression. Importance in the metabolic control of diabetes. N. Engl. J. Med. *299*, 433–436. https://doi.org/10.1056/nejm197808312990901.

Reaven, G.M., Chen, Y.D., Golay, A., Swislocki, A.L., and Jaspan, J.B. (1987). Documentation of hyperglucagonemia throughout the day in nonobese and obese patients with noninsulin-dependent diabetes mellitus. J. Clin. Endocrinol. Metab. *64*, 106–110. https://doi.org/10.1210/jcem-64-1-106.

Richter, M.M., Galsgaard, K.D., Elmelund, E., Knop, F.K., Suppli, M.P., Holst, J.J., Winther-Sørensen, M., Kjeldsen, S.A.S., and Wewer Albrechtsen, N.J. (2022). The liver-alpha-cell Axis in health and in disease. Diabetes *71*, 1852–1861. https://doi.org/10.2337/dbi22-0004.

Schneider, C.A., Rasband, W.S., and Eliceiri, K.W. (2012). NIH Image to ImageJ: 25 years of image analysis. Nat. Methods *9*, 671–675. https://doi.org/10.1038/nmeth.2089.

Snodgrass, P.J., Lin, R.C., Müller, W.A., and Aoki, T.T. (1978). Induction of urea cycle enzymes of rat liver by glucagon. J. Biol. Chem. *253*, 2748–2753. https://doi.org/10.1016/S0021-9258(17)40885-4.

Solloway, M.J., Madjidi, A., Gu, C., Eastham-Anderson, J., Clarke, H.J., Kljavin, N., Zavala-Solorio, J., Kates, L., Friedman, B., Brauer, M., et al. (2015). Glucagon couples hepatic amino acid catabolism to mTOR-dependent regulation of alpha-cell mass. Cell Rep. *12*, 495–510. https://doi.org/10.1016/j.celrep.2015.06.034.

Spijker, H.S., Ravelli, R.B.G., Mommaas-Kienhuis, A.M., Van Apeldoorn, A.A., Engelse, M.A., Zaldumbide, A., Bonner-Weir, S., Rabelink, T.J., Hoeben, R.C., Clevers, H., et al. (2013). Conversion of mature human beta-cells into glucagon-producing alpha-cells. Diabetes *62*, 2471–2480. https://doi.org/10.2337/db12-1001.

Suppli, M.P., Bagger, J.I., Lund, A., Demant, M., Van Hall, G., Strandberg, C., Kønig, M.J., Rigbolt, K., Langhoff, J.L., Wewer Albrechtsen, N.J., et al. (2020). Glucagon resistance at the level of amino acid turnover in obese subjects with hepatic steatosis. Diabetes *69*, 1090–1099. https://doi.org/10.2337/db19-0715.

Thoden, J.B., Wesenberg, G., Raushel, F.M., and Holden, H.M. (1999). Carbamoyl phosphate synthetase: closure of the B-domain as a result of nucleotide binding. Biochemistry *38*, 2347–2357. https://doi.org/10.1021/bi982517h.

Tillner, J., Posch, M.G., Wagner, F., Teichert, L., Hijazi, Y., Einig, C., Keil, S., Haack, T., Wagner, M., Bossart, M., and Larsen, P.J. (2019). A novel dual glucagon-like peptide and glucagon receptor agonist SAR425899: results of randomized, placebo-controlled first-in-human and first-in-patient trials. Diabetes Obes. Metabol. *21*, 120–128. https://doi.org/10.1111/dom.13494.

Vega, R.B., Whytock, K.L., Gassenhuber, J., Goebel, B., Tillner, J., Agueusop, I., Truax, A.D., Yu, G., Carnero, E., Kapoor, N., et al. (2021). A metabolomic signature of glucagon action in healthy individuals with overweight/obesity. J. Endocr. Soc. *5*, bvab118. https://doi.org/10.1210/jendso/bvab118.

Watanabe, C., Seino, Y., Miyahira, H., Yamamoto, M., Fukami, A., Ozaki, N., Takagishi, Y., Sato, J., Fukuwatari, T., Shibata, K., et al. (2012). Remodeling of hepatic metabolism and hyperaminoacidemia in mice deficient in proglucagon-derived peptides. Diabetes *61*, 74–84. https://doi.org/10.2337/db11-0739.

Wewer Albrechtsen, N.J., Junker, A.E., Christensen, M., Hædersdal, S., Wibrand, F., Lund, A.M., Galsgaard, K.D., Holst, J.J., Knop, F.K., and Vilsbøll, T. (2018). Hyperglucagonemia correlates with plasma levels of non-branched-chain amino acids in patients with liver disease independent of type 2 diabetes. Am. J. Physiol. Gastrointest. Liver Physiol. *314*. G91–g96. https://doi.org/10.1152/ajpgi.00216.2017.

Wewer Albrechtsen, N.J., Kuhre, R.E., Toräng, S., and Holst, J.J. (2016a). The intestinal distribution pattern of appetite- and glucose regulatory peptides in mice, rats and pigs. BMC Res. Notes *9*, 60. https://doi.org/10.1186/s13104-016-1872-2.

Wewer Albrechtsen, N.J., Kuhre, R.E., Windeløv, J.A., Ørgaard, A., Deacon, C.F., Kissow, H., Hartmann, B., and Holst, J.J. (2016b). Dynamics of glucagon secretion in mice and rats revealed using a validated sandwich ELISA for small sample volumes. Am. J. Physiol. Endocrinol. Metab. *311*, E302–E309. https://doi.org/10.1152/ajpendo.00119.2016.

Winther-Sørensen, M., Galsgaard, K.D., Santos, A., Trammell, S.A.J., Sulek, K., Kuhre, R.E., Pedersen, J., Andersen, D.B., Hassing, A.S., Dall, M., et al. (2020). Glucagon acutely regulates hepatic amino acid catabolism and the effect may be disturbed by steatosis. Mol. Metab. *42*, 101080. https://doi.org/10.1016/j.molmet.2020.101080.

Yu, G., Wang, L.G., Han, Y., and He, Q.Y. (2012). clusterProfiler: an R package for comparing biological themes among gene clusters. OMICS *16*, 284–287. https://doi.org/10.1089/omi.2011.0118.

STAR★METHODS

KEY RESOURCES TABLE

REAGENT or RESOURCE	SOURCE	IDENTIFIER
Antibcodies		
REGN1193	Regeneron	RRID: AB_2783540
Goat Anti-rabbit	Vector Laboratories	Cat# BA-1000; RRID:AB: 2313606
Goat Anti-guinea pig	Vector Laboratories	Cat# BA-7000; RRID:AB: 2336132
Chemicals, peptides, and recombinant proteins		
NNC9204-0043	This paper	N/A
Tissue-Tek® Tissue-Clear® Xylene Substitute	Gentaur	Cat# 94–1466
Avidin and Biotinylated horseradish peroxidase macromolecular Complex	Vector Laboratories	Cat# PK-6100
3,3-diaminobenzidine	Vector Laboratories	SK-4105
Acetonitrile (hypergrade for LC-MS)	Sigma-Aldrich	Cat# 10000292500
Methanol (UHPLC for MS)	Sigma-Aldrich	Cat# 9006881L
Water LC-MS Grade	Sigma-Aldrich	Cat# 1153332500
Amino acid isotopologoues	Cambridge Isotope Laboratories	Cat# MSK-A2-1.2
[$^{13}C_5$]-L-glutamine	Sigma-Aldrich	Cat# 605166
[$^{2}H_5$]-D-tryptophan	CDN Isotopes	Cat# D-7416
Amino acid standard	Sigma-Aldrich	Cat# AAS18
L-Alanine	Sigma-Aldrich	Cat# 05130
L-Asparagine	Sigma-Aldrich	Cat# A0884
L-Glutamine	Sigma-Aldrich	Cat# G8540
L-Threonine	Sigma-Aldrich	Cat# T8441
L-Tryptophan	Sigma-Aldrich	Cat# T0254
Critical commercial assays		
Glucagon ELISA	Mercodia	Cat# 10-1281-01
Insulin ELISA	Mercodia	Cat# 10-1247-01
L-Amino Acid Assay Kit	Abcam	Cat# ab65347
QuantiChrom Urea Assay Kit	BioAssay Systems	Cat# DIUR-100
AllPrep DNA/RNA Minikit	QIAgen	Cat# 80204
RNeasy Minikit	QIAgen	Cat# 74106
RNase-Free DNase set	QIAgen	Cat# 79254
TruSeq Stranded Total RNA Library Prep Gold	Illumina	Cat# 20020599
IDT for Illumina TruSeq RNA UD Indexes	Illumina	Cat# 20022371
NEBNext Ultra II Directional RNA Library Prep Kit for Illumina	New England Biolabs	NEB-E7760S
NEBNext rRNA Depletion Kit 24	New England Biolabs	NEB-E7765
NEBNext Multiplex Oligos for Illumina	New England Biolabs	E7600S
Deposited data		
R Code	This paper	https://doi.org/10.5281/zenodo.7016693
Experimental models: Organisms/strains		
Mouse: C57BL/6JRj	Janvier Laboratories	RRID:MGI:2670020
Mouse: *Gcgr*$^{-/-}$	Gelling et al. (2003)	N/A

(*Continued on next page*)

Continued

REAGENT or RESOURCE	SOURCE	IDENTIFIER
Software and algorithms		
Fiji ImageJ	Schneider et al. (2012)	https://imagej.nih.gov/ij/download.html RRID:SCR_003070
bcl2fastq software version 2.20.0	Illumina	https://support.illumina.com/sequencing/sequencing_software/bcl2fastq-conversion-software.html RRID:SCR_015058
FastQC version 0.11.9	Babraham Bioinformatics	https://www.bioinformatics.babraham.ac.uk/projects/fastqc/ RRID:SCR_014583
Salmon version 1.6.0	Patro et al. (2017)	RRID:SCR_017036
GraphPad version 9.2.0	Graphpad Software	RRID:SCR_002798
DESeq2 version 1.34.0	Anders and Huber (2010)	RRID:SCR_015687
Other		
App of differentially expressed genes in GCGA-treated mice	This paper	https://doi.org/10.5281/zenodo.7016868
App of differentially expressed genes in GCGR Ab-treated mice	This paper	https://doi.org/10.5281/zenodo.7016891
App of differentially expressed genes in *Gcgr*$^{-/-}$ mice	This paper	https://doi.org/10.5281/zenodo.7016909

RESOURCE AVAILABILITY

Lead contact

Nicolai J. Wewer Albrechtsen nicolai.albrechtsen@sund.ku.dk.

Further information and requests for resources and reagents should be directed to and will be fulfilled by the lead contact, Nicolai J. Wewer Albrechtsen.

Materials availability

We developed three apps, in which data on all the genes analyzed for differential expression can be found, visualized, and downloaded. These apps are publicly available at: https://weweralbrechtsenlab.shinyapps.io/GCGA/, https://weweralbrechtsenlab.shinyapps.io/GCGR_Ab/ and https://weweralbrechtsenlab.shinyapps.io/GcgrKO/.

This paper must be cited if data from the abovementioned apps are used, presented, or published. This study did not generate new unique reagents.

Data and code availability

- All data reported in this paper will be shared by the lead contact upon request. All RNA sequencing results generated are available through our apps as of the date of publication, DOIs are listed in the key resources table. RNA sequencing data are available at https://www.ebi.ac.uk/biostudies/ under the accession numbers; **GCGA**: E-MTAB-12040, **GCGR Ab:** E-MTAB-12048, and **GCGR KO:** E-MTAB-12060
- All original code has been deposited www.github.com/nicwin98 and is publicly available as of the date of publication. DOIs are listed in the key resources table.
- Any additional information required to reanalyze the data reported in this paper is available from the lead contact upon request.

EXPERIMENTAL MODEL AND SUBJECT DETAILS

Animals

Animal studies were conducted with permission from the Danish Animal Experiments Inspectorate, license no. 2018-15-0201–01397, in accordance with the EU directive 2010/63/EU and guidelines of Danish legislation governing animal experimentation (1987), and the US Institutes of health (publication number 85–23). The studies were approved by the local ethical committee (P21-337). Female C57BL/6JRj mice were obtained from Janvier Laboratories, Saint-Berthevin Cedex, France. Female and male *Gcgr*$^{-/-}$ and wild-type (*Gcgr*$^{+/+}$) littermates were from in-house breeding (previously described in (Gelling et al., 2003)). All mice were housed in ventilated cages in groups of 4–8 mice per cage and fed standard chow and water *ad libitum*. The mice followed a 12-h light cycle with lights on from 6 AM to 6 PM. All mice were acclimatized for at least one week before starting experiments.

Treatment

For eight weeks, female C57BL/6JRj mice (seven weeks old at the start of treatment) received, by subcutaneous injections, either a long-acting glucagon analog(GCGA, NNC9204-0043, Novo Nordisk A/S, 1.5 nmol/kg body weight, terminal half-life: 5–6 h), PBS +1% BSA (PBS), a glucagon receptor antibody (GCGR Ab, REGN1193, 10 mg/kg body weight; Regeneron; IC_{50}: 3.5 pM (Okamoto et al., 2015)) or a control antibody (Ctl Ab, REGN1945, 10 mg/kg body weight; Regeneron). The antibodies and the glucagon analogwere dissolved in PBS +1% BSA. Dose and administration frequency of GCGA was determined in a pilot study, in which 3 nmol/kg or 30 nmol/kg GCGA or PBS was administered to male and female C57BL/6JRj mice (8 weeks old) once or twice during a 24 h period. The antibodies (GCGR Ab and Ctl Ab) were administered once weekly (Wednesdays at 8 AM), while GCGA and PBS were administered twice daily (at 8 AM and 8 PM). To monitor the health of the mice, they were weighed, and blood glucose was measured with a handheld glucometer (Accu-Chek® Mobile, Roche Diagnostics) each Wednesdays at 8 AM prior to injections. The dose of GCGA was initially 3 nmol/kg body weight, but after 16 days of treatment, one of the mice had lost >20% of its body weight and had to be terminated (this mouse was excluded from the study). Due to this effect of GCGA, the dose was halved (1.5 nmol/kg body weight) for the remainder of the study. Prior to the first injection (baseline) and after four weeks of treatment, a blood sample (~150 μL) was taken from the retroorbital plexus in ethylenediaminetetraacetic acid (EDTA)-coated capillary tubes (Vitrex Medical A/S, Herlev, Denmark). Blood samples were centrifuged at 4000 × *g*, 4°C, 10 min, and plasma was collected and stored at −80°C until biochemical analyses. The mice were treated for a total of eight weeks, fasted overnight (11 h from 10 PM to 9 AM) and then killed by cervical dislocation, and the pancreas and liver were isolated and weighed. A biopsy of pancreas was fixated in 4% paraformaldehyde, and the rest as well as a liver biopsy were snap-frozen in liquid nitrogen and subsequently stored at −80°C. The last doses of GCGA and PBS were given 16 h prior to termination, and the last doses of GCGR Ab and Ctl Ab were given one week prior to termination.

METHOD DETAILS

Preparation of the long-acting glucagon analog, GCGA, NNC9204-0043

The glucagon analogNNC9204-0043 (GCGA, Novo Nordisk A/S, see Figure S1) was prepared by solid phase peptide synthesis using Fmoc based chemistry on a Prelude Solid Phase Peptide Synthesizer (Protein Technologies) on a preloaded Fmoc(Thr(tBu)-Wang resin. The glucagon analogue had the following sequence substitutions: 17K, 18K, 21E, 24K(2xOEGgGlu-C18 diacid), 27L. Introduction of the substituent on the epsilon-nitrogen of a lysine was achieved using a lysine protected with Mtt (Fmoc-Lys(Mtt)-OH). The Mtt group was removed using HFIP/DCM/TIPS (75:20:5) (5 min). Cleavage of peptide from the resin were achieved using (TFA/TIPS/H2O (95:2.5:2.5 vol/vol) for 2.5h). The crude peptides were purified by reversed-phase preparative HPLC (Waters Delta Prep 4000) on a column comprising C18-silica gel. Elution was performed with an increasing gradient of MeCN in MQ water comprising 0.1% trifluoroacetic acid. The fractions were then analyzed by UPLC and LCMS and pure fractions were combined and freeze dried.

Biochemical analyses

Plasma concentrations of glucagon were measured using a two-site enzyme immunoassay (10-1281-01, Mercodia). This assay was used to measure plasma concentrations of glucagon (using WHO calibrated glucagon as standards) upon GCGA administration as this assay also detects GCGA. Plasma concentrations of insulin were measured using a two-site enzyme immunoassay (10-1247-01, Mercodia). Plasma concentrations of total L-amino acids were measured using an enzymatic assay (ab65347, Abcam), and plasma

concentrations of urea were quantified using QuantiChrom Urea Assay Kit (DIUR-100, BioAssay Systems). Peptides were extracted from pancreatic tissue biopsies using trifluoroacetic acid, as previously described (Wewer Albrechtsen et al., 2016a) and after centrifugations and desiccation of the supernatant, concentrations of insulin and glucagon were measured in the reconstituted extracts using radioimmunoassays (antiserum 4305 for glucagon and antiserum 2006–3 for insulin). For measurement of CPS-1 activity, liver biopsies were homogenized in a buffer containing 10 mM HEPES, pH 7.4, 0.5% Triton X-100, 2 mM dithiothreitol and centrifuged at 13,000 × *g*, 4°C for 5 min. CPS-1 enzyme activity was measured in the supernatant using a colorimetric assay, as previously described (Pierson, 1980). Briefly, 20 μL protein samples (~1 μg/uL) were added to 200 μL of an enzymatic reaction mixture (containing 50 mM ammonium icarbonate, 5 mM ATP, 10 mM magnesium acetate, 5 mM n-acetyl-l-glutamate, 1 mM dithiotreitol, and 50 mM triethanolamine) and incubated for 10 min at 37°C. Next, 10 μL 2 M hydroxylamine was added, and the samples were incubated for 10 min at 95°C. Finally, a chromogenic mixture of equal amounts of 0.045 M antipyrine in 40% sulfuric acid (vol/vol) and 0.06 M butamedione monoxime in 5% acetic acid (vol/vol) was prepared, and 800 μL of the mix was added to the samples, which were incubated for 15 min at 95°C. After cooling down to room temperature, absorbance was measured at 458 nm.

Histology

The pancreas samples were fixed in 4% paraformaldehyde for 24 h and then transferred to 70% ethanol. The tissues were prepared in a vacuum tissue processer (Shandon Exelsior; Thermo Fisher Scientific) overnight and embedded into paraffin. The samples were cut in sections of 4 μm and dewaxed through Tissue-Clear (Tissue-Tek® Tissue-Clear® Xylene Substitute, 94–1466, Gentaur). For antigen retrieval, the sections were boiled in a microwave oven for 15 min in EGTA-buffer, pH 9, pre-incubated in 2% BSA for 10 min and then incubated for one hour at room temperature with the primary antibody diluted in 2% BSA. In-house antibodies for glucagon (4304, 1:15,000, made in rabbits), insulin (2006, 1:30,000, made in guinea pigs), and somatostatin (1759, 1:15,000, made in rabbits) were used. The sections were incubated for 40 min with a second layer of biotinylated secondary antibody immunoglobins 1:200 (For glucagon and somatostatin: Goat anti-Rabbit, BA-1000; for insulin: Goat anti-guinea pig, BA-7000; Vector Laboratories), followed by addition of 3% hydrogenperoxide to block endogenous peroxidase. The third layer was formed by a preformed Avidin and Biotinylated horseradish peroxidase macromolecular Complex (Elite ABC, PK-6100, Vector Laboratories) for 30 min. Finally, the reaction was developed with 3,3–diaminobenzidine (DAB+, SK-4105, Vector Laboratories) for 15 min, and counterstaining was performed with Mayers Hematoxylin. The immunohistochemistry stainings were performed on Autostainer link 48 DAKO. Analysis of stained area was done in ImageJ (Schneider et al., 2012). Images were converted to 8-bits, saturated pixels were set to 0.4% and the contrasts were colored red. An islet was traced with the free-hand tool, and the immunoreactive (red) area in each islet quantified.

Plasma amino acid quantitation via liquid chromatography-mass spectrometry

Unless otherwise stated, all solvents were of liquid chromatography-mass spectrometry (LC-MS) grade purity. 2.5 μL of plasma was added to 97.5 μL of a pre-cooled (−20°C) mixture (2:2:1 (v/v/v)) of acetonitrile (hypergrade for LC-MS, 10000292500, Sigma-Aldrich), methanol (UHPLC for MS, 9006881L, Sigma-Aldrich), and water (LC-MS Grade, 1153332500, Sigma-Aldrich). The acetonitrile:methanol:water mixture contained internal standards in the form of isotopologues of each amino acid (MSK-A2-1.2, Cambridge Isotope Laboratories), except for L-asparagine and L-tryptophan, for which [$^{13}C_5$]-L-glutamine (605166, Sigma-Aldrich) and [$^{2}H_5$]-D-tryptophan (D-7416, CDN Isotopes, Canada) were used (See Table S4). The mixture contained 62.5 pmol of the [$^{13}C^6$, $^{15}N_2$]-L-cystine standard and 125 pmol of all other standards. The mixtures were vortexed, left standing at −20°C for 30 min and then centrifuged at 13,000 × *g* without temperature control for 5 min. 80 μL of supernatant was transferred to a fresh autosampler vial. 5 μL of each extract were pooled to serve as the quality control (QC). A blank extract was prepared by replacing the volume of plasma with demineralized water. Four pooled human plasma samples from healthy individuals were also extracted to serve as plasma QCs. In addition, standard QCs (0.24, 8 and 40 pmol) and external standards (0.005, 0.01, 0.05, 0.1, 0.3, 1, 3, 10, 15, 30, 37.5, 50, 150, and 200 pmol, AAS18, 05130, A0884, G8540, T8441, T0254, Sigma-Aldrich) were prepared with the same amount of internal standard as used for the samples.

Samples were injected in a random order. The QC pooled sample was injected six times at the beginning of the analysis, twice after half of the samples were injected, and twice after all samples were injected. The QC standards were injected after each QC pooled sample injection series. The standard curve was injected after all samples had been injected. All samples, the QC pooled sample, the blank, the QC standards, and

the standard curve were injected (2 μL) into a Waters ACQUITY UPLC I-Class PLUS System and separated using liquid chromatography. Amino acids were separated over an Imtakt Intrada Amino Acid column (2.1 × 100 mm, 3 μm) heated at 35°C using a gradient between mobile phase A (100 mM ammonium formate in water) and mobile phase B (acetonitrile/water(95%/5% (v/v)) and 0.3% (v/v) formic acid) at a flow rate of 0.3 mL/min. The gradient was as described in (Liu et al., 2019). Electrospray generated ions were analyzed using a Waters Xevo TQ-XS mass spectrometer operated in positive, multiple-reaction monitoring mode. The following mass spectrometry conditions were used: capillary voltage = 3 kV, source temperature = 150°C, desolvation temperature = 600°C, cone nitrogen flow = 150 L/h, collision argon flow = 0.15 mL/min, and nebulizer nitrogen flow = 7 bar. Transitions are described in Table S4. Quantities were determined using an internally controlled calibration curve with 1/X2 weighting. Results were converted to μM from pmol by relating the total pmol in a sample to the volume of plasma extracted.

RNA sequencing

Liver biopsies were taken from mice treated for eight weeks with GCGA, PBS, GCGR Ab, or Ctl Ab. The mice were fasted overnight (11 h) prior to liver isolation, as described above, and livers were kept at −80°C until analysis. Total DNA/RNA was purified by an AllPrep DNA/RNA Minikit (80204, QIAgen) according to manufacturer's instructions and quality tested using a 2100 Bioanalyzer instrument (Agilent Genomics). The extract was Dnase treated with Rneasy Minikit (74106, QIAgen) and Rnase-Free Dnase set (79254, QIAgen) according to manufacturer's protocol. All the above-mentioned processes were performed on a QIACube machine (QIAgen). Library preparation was done using TruSeq Stranded Total RNA Library Prep Gold (20020599, Illumina) and IDT for Illumina-TruSeq RNA UD Indexes (20022371, Illumina) according to the manufacturer's instructions. Some samples (input <100 ng) were prepared with NEBNext Ultra II Directional RNA Library Prep Kit for Illumina (NEB-E7760S, New England Biolabs), NEBNext rRNA Depletion Kit 24 with beads (NEB-E7765, New England Biolabs), and NEBNext Multiplex Oligos for Illumina (E7600S, New England Biolabs). RNA sequencing libraries were paired-end sequenced (2 x 150 bp) on an Illumina Novaseq 6000 instrument using a S1 flow cell and raw sequencing data were processed using bcl2fastq software version 2.20.0 (Illumina).

Bioinformatic analysis of RNA sequencing data

The read quality of the raw sequencing data (FASTQ) was evaluated using FastQC version 0.11.9. Reads were mapped to a decoy-aware transcriptome (M28/GRCm39) using Salmon version 1.6.0 (Patro et al., 2017) and selective alignment. The data were normalized using the algorithm variance stabilizing transformation offered by the DESeq2 package (Anders and Huber, 2010) version 1.34.0 in R version 4.1.0. The same R package was used to identify differentially expressed genes (FDR<0.05). Raw sequencing data for liver samples from male *Gcgr*$^{-/-}$ mice (Winther-Sorensen et al., 2020) were re-analyzed using the bioinformatic analysis presented above. This was done to minimize potential biases when comparing the transcriptome profile of *Gcgr*$^{-/-}$ mice and GCGR Ab mice. Differentially expressed genes related to amino acid processes were filtered using Gene Ontology (GO) (Ashburner et al., 2000; Gene Ontology Consortium, 2021) annotations for the umbrella terms "Cellular amino acid metabolic process", "Amino acid transport", "Amino acid homeostasis", "Response to amino acid", and all *child terms*. . GO.db: A set of annotation maps describing the entire Gene Ontology. R package version 3.8.2] (Yu et al., 2012; Carlson, 2022).

QUANTIFICATION AND STATISTICAL ANALYSIS

Statistical calculations and graphs were made using GraphPad Prism version 9.2.0 (GraphPad Software). Data are reported as mean ± SEM or mean ± SD as indicated. With the exception of RNA sequencing data, significance was assessed by two-way ANOVA corrected for multiple testing using Holm-Sidak correction, paired or unpaired t-tests as indicated with significance levels: *p < 0.05, **p < 0.01, ***p < 0.001, ****p < 0.0001.